Cerebellar degeneration reduces memory resilience after extended training

Thomas Hulst[1,2,3*], Ariels Mamlins[1], Maarten Frens[3], Dae-In Chang[1], Sophia L. Göricke[4], Dagmar Timmann[1#], Opher Donchin[5#]

[1] Department of Neurology, Essen University Hospital, University of Duisburg-Essen, 45122 Essen, Germany

[2] Erasmus University College, 3011 HP Rotterdam, The Netherlands

[3] Department of Neuroscience, Erasmus MC, 3000 CA Rotterdam, The Netherlands

[4] Department of Diagnostic and Interventional Radiology and Neuroradiology, Essen University Hospital, University of Duisburg-Essen, 45122 Essen, Germany

[5] Department of Biomedical Engineering, Zlotowski Center for Neuroscience, Ben-Gurion University of the Negev, Beer-Sheva 8410501, Israel

[#] Authors contributed equally to this work.

[*] Corresponding author at: Erasmus University College, Nieuwemarkt 1A, 3011 HP, Rotterdam, E-mail address: hulst@euc.eur.nl (Thomas Hulst)

Conflict of interest statement: The authors declare no competing financial interests.

Acknowledgements: The study was funded by a grant of the German Research Foundation (DFG TI 239/16-1) awarded to OD and DT and a scholarship from the **E**ssener Ausbildungsprogramm "**L**abor und Wissenschaft" für den **A**erztlichen **N**achwuchs (ELAN) supported by the Else Kröner-Fresenius-Stiftung awarded to AM. We would like to thank Beate Brol for her support in the analysis of this experiment.

Abstract

Patients with cerebellar ataxia suffer from various motor learning deficits hampering their ability to adapt movements to perturbations. Motor adaptation is hypothesized to be the result of two subsystems: a fast learning mechanism and a slow learning mechanism. We tested whether training paradigms that emphasize slow learning could alleviate motor learning deficits of cerebellar patients. Twenty patients with cerebellar degeneration and twenty age-matched controls were trained on a visuomotor task under four different paradigms: a standard paradigm, gradual learning, overlearning and long intertrial interval learning. Expectedly, cerebellar participants performed worse compared to control participants. However, both groups demonstrated elevated levels of spontaneous recovery in the overlearning paradigm, which we saw as evidence for enhanced motor memory retention after extended training. Behavioral differences were only found between the overlearning paradigm and standard learning paradigm in both groups.

Modelling suggested that, in control participants, additional spontaneous recovery was the result of higher retention rates of the slow system as well as reduced learning rates of the slow system. In cerebellar participants however, additional spontaneous recovery appeared only to be the result of higher retention rates of the slow system and not reduced learning rates of the slow system. Thus, memory resilience was reduced in cerebellar participants and elevated levels of slow learning were less resilient against washing out. Our results suggest that cerebellar patients might still benefit from extended training through use-dependent learning, which could be leveraged to develop more effective therapeutic strategies.

1 Introduction

The cerebellar ataxias are a heterogeneous group of disorders clinically identified by cerebellar dysfunction. Patients exhibit a range of impairments in motor control, including incoordination of eye movements, dysarthria, limb incoordination, and gait disturbances (Mariotti et al., 2005), as well as impairments in the cognitive domain (Schmahmann and Sherman, 1998). While the genetic and pathophysiological underpinnings of many of the cerebellar ataxias are increasingly well understood (Jayadev and Bird, 2013; Matilla-Dueñas et al., 2014), treatment remains a major challenge with genetic therapies being at the horizon for only a subset of genetically defined ataxias (Scoles et al., 2017). Contemporary cerebellar therapy is aimed at alleviating motor symptoms to maintain activities of daily living (ADL), as no curative therapy currently exists (Ilg et al., 2014). Although the consensus is that cerebellar patients benefit from supportive therapy, i.e. physical therapy, speech therapy and occupational therapy, little is known about the mechanisms underlying the improvements and how patients can benefit most (Fonteyn et al., 2014; Ilg et al., 2014). Providing effective care for ataxia patients can be especially challenging, since cerebellar patients suffer from various motor learning deficits (Maschke et al., 2004; Tseng et al., 2007) and initial studies suggest a relationship between motor learning deficits and the efficacy of neurorehabilitation programs (Hatakenaka et al., 2012). An intervention which can lessen these motor learning deficits might therefore augment the effects of cerebellar therapy.

Previous work has found that motor learning deficits of cerebellar patients can partially be ameliorated when trained with an explicit strategy (Taylor et al., 2010) or by altering the type of feedback (Therrien et al., 2016). There is also limited evidence that training paradigms that emphasize slow learning processes might alleviate motor learning deficits (Criscimagna-Hemminger et al., 2010), but, as of yet, few studies have examined this notion. Early evidence pointed to beneficial effects of the gradual introduction of reaching movement perturbations

in cerebellar patients (Criscimagna-Hemminger et al., 2010), but this was not replicated in cerebellar patients in subsequent work (Gibo et al., 2013; Schlerf et al., 2013). On the other hand, in studies with healthy individuals, training paradigms which emphasize slow learning have shown robust effects on motor performance. For instance, when healthy individuals keep training after attaining asymptotic performance on a motor learning task, so-called overlearning, retention increases with the number of trials trained at the asymptote (Joiner and Smith, 2008). The amount with which retention increases can be predicted by a two-state model that incorporates a fast and slow learning mechanism and is thought to be the result of increased engagement of the slow state of motor learning (Joiner and Smith, 2008; Smith et al., 2006). Similarly, when healthy individuals train with long intertrial intervals (ITI) between movements, the rate of learning decreases, but retention increases due to more trial-to-trial forgetting of the fast state of motor learning and more activation of the slow state of motor learning (Kim et al., 2015; Sing et al., 2009).

The aim of the present study was to study slow learning processes in more detail, in particular in patients with cerebellar degeneration, and to assess whether paradigms that emphasize slow learning affect behavioral measures of motor learning. We tested twenty patients with degenerative ataxia and twenty healthy age- and sex-matched controls on a visuomotor reaching adaptation task under four different training paradigms (a standard learning paradigm, gradual learning, overlearning and long intertrial interval (ITI) learning). The paradigms, other than the standard learning paradigm, were specifically chosen to stimulate slow learning in individuals.

We expected to find impaired motor learning in cerebellar participants under a standard training paradigm, characterized by incomplete adaptation to visuomotor perturbations and decreased retention. Training cerebellar participants with paradigms that emphasize slow learning might enable them to compensate for these motor learning deficits. If slow learning

92 paradigms allow cerebellar participants to compensate motor learning deficits, it could

93 facilitate the design of new strategies in supportive therapy.

2 Methods

2.1 Participants

Twenty participants with cerebellar degeneration (9 females, 54.9 years ± 10.8 (SD), range 18 – 70 years) and twenty age- and sex-matched participants (9 females, 55.2 years ± 11.2 (SD), range 18 – 71 years), took part in the study. Cerebellar participants were recruited from the patients attending our ataxia clinic and matched controls were recruited via print advertisements distributed on the hospital campus. Only right-handed individuals were included, as assessed by the Edinburgh Handedness Inventory (Oldfield, 1971). The severity of cerebellar symptoms in the group of cerebellar participants was assessed by one experienced neurologist (DT) and healthy age- and sex-matched controls were examined by AM. Cerebellar symptoms were scored on the International Cooperative Ataxia Rating Scale (ICARS; Trouillas et al., 1997), as well as the Scale for the Assessment and Rating of Ataxia (SARA; Schmitz-Hübsch et al., 2006). The group of cerebellar participants was diagnosed with diseases known to primarily affect the cerebellar cortex (Gomez et al., 1997; Timmann et al., 2009). Three age-matched controls were excluded and replaced due to neurological symptoms on their examination or minor extracerebellar pathology on their MRI. All participants gave informed oral and written consent. The experiment was approved by the ethics committee of the medical faculty of the University of Duisburg-Essen and conducted in accordance with the Declaration of Helsinki. The characteristics of the recruited cerebellar participants and matched controls can be found in **Table 1**.

Table 1

Overview Cerebellar participants and Control participants

Cerebellar participants							**Control participants**		
ID	**Age**	**Sex**	**Diagnosis**	**Disease duration**	**ICARS** (total/100)	**SARA** (total/40)	**ID**	**Age**	**Sex**

P01	18	M	ADCAIII	18 years	10.5	5	C01	18	M
P02	47	M	ADCAIII	25+ years	40	17.5	C02	43	M
P03	50	F	ADCAIII	25+ years	31	11.5	C03	50	F
P04	51	M	SCA14	25+ years	31	11.5	C04	50	M
P05	51	F	ADCAIII	19 years	29	12.5	C05	51	F
P06	52	F	SCA14	22 years	26.5	12	C06	53	F
P07	53	F	SCA6	2 years	23	9.5	C07	54	F
P08	53	M	SAOA	17 years	40	15	C08	53	M
P09	53	M	ADCAIII	17 years	36	11	C09	51	M
P10	54	F	SCA6	4 years	30.5	10	C10	56	F
P11	56	F	SCA14	25+ years	28	12	C11	58	F
P12	57	M	SCA6	11 years	38	11	C12	53	M
P13	57	M	SCA6	15 years	28	8	C13	59	M
P14	58	M	SAOA	25+ years	63.5	22	C14	61	M
P15	59	M	SCA6	5 years	23	9.5	C15	63	M
P16	60	F	SCA6	11 years	36.5	14	C16	60	F
P17	63	F	ADCAIII	23 years	33	13.5	C17	66	F
P18	66	M	SAOA	13 years	24.5	11	C18	66	M
P19	70	F	SAOA	7 years	32.5	12.5	C19	71	F
P20	70	M	SAOA	16 years	38	15	C20	67	M

Table 1: *Cerebellar participants were age- and sex-matched with the controls on the right side of the table. SCA6 = spinocerebellar ataxia type 6; SCA14 = spinocerebellar ataxia type 14; SAOA = sporadic adult onset ataxia; ADCA III = autosomal dominant ataxia type III; ICARS = International Cooperative Ataxia Rating Scale (Trouillas et al., 1997); SARA = Scale for the Assessment and Rating of Ataxia (Schmitz-Hübsch et al., 2006). Disease duration is years since presentation of the first symptoms.*

2.2 Task

All participants completed a standard reaching task with visuomotor perturbations. The experimental setup and task have been described previously in other studies from our group (Rabe et al., 2009). In short, participants were seated in front of an upright monitor and could, with their right hand, move a two-jointed manipulandum freely in the horizontal plane (**Figure 1A**). Vision of the participant's arm was obstructed by a black cloth. Hand position and velocities were measured in a resolution of 10^6 counts per revolution and a sampling rate of 200 Hz (DMC-1826; Galil Motion Control). The location of the participant's hand was represented on the monitor by a green dot with a diameter of 5 mm. The origin and target

128 locations were represented by a circle with a diameter of 10 mm, colored red and white
129 respectively. At the start of each trial, the participant's hand was moved towards the origin
130 location by the servomotors connected to the manipulandum. Then, after a delay of 2000ms, a
131 target circle appeared at one of three possible target locations, located 10 centimeters away
132 from the origin at an angle of 66°, 90° or 114° (**Figure 1B**). Participants were instructed to
133 move the green dot from the origin towards the target with a "quick and accurate movement"
134 as soon as the target appeared. When participants moved the cursor through an invisible
135 boundary located 10 centimeters from the origin, their hand was gently brought to a stop by a
136 simulated cushion, indicating the end of the movement. Following each movement,
137 participants received feedback on whether they hit the target and moved with the correct
138 velocity. The target turned yellow when moving too fast, blue when moving too slow, and
139 green when moving with the correct velocity. Participants moved with the correct velocity
140 when their movement and reaction time fell within a 250ms window centered around 500ms.
141 The 250ms window shrunk by 10% every time a movement had the correct velocity and
142 increased by 10% when moving too fast or slow, adapting to a participant's individual
143 capabilities. When participants also managed to hit the target, in addition to moving with the
144 correct velocity, a "yahoo" sound was played.

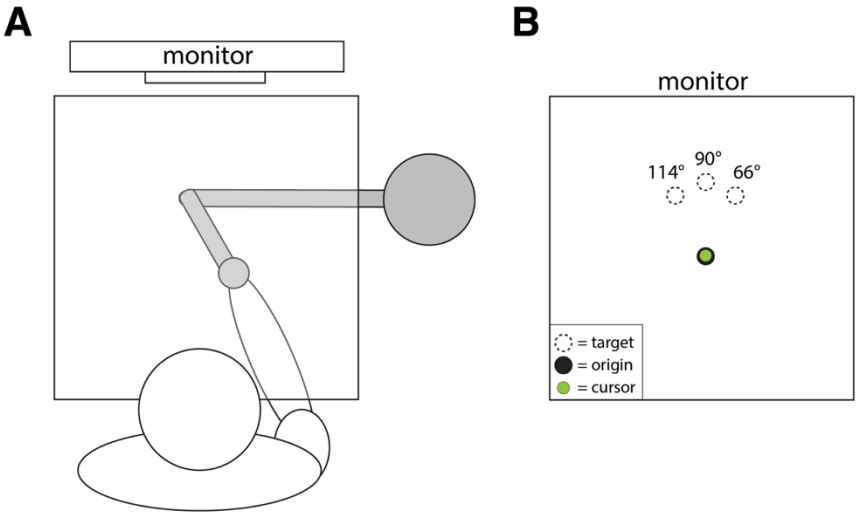

145

***Figure 1**: A) Experimental setup. For illustrative purposes the tabletop is pictured here as transparent. In reality the tabletop was opaque to obstruct the view of the hand and robot arm. Additionally, a black cloth was draped over the shoulders of the participant and attached to the table to obstruct vision of the arm. B) Localization of origin and target circles on the monitor. One of the three target circles would pseudo-randomly appear at the start of a movement trial.*

The experimental task consisted of 4 different training paradigms. Each paradigm consisted of a baseline set, an adaptation set, and a washout set. All participants completed each of the training paradigms. The order of paradigms was counterbalanced with a Latin-squares design against first-order carryover effects (Williams, 1949). Every paradigm order was completed by 10 participants each (five cerebellar participants and five control participants) (**Figure 2A**). Furthermore, perturbation direction in the adaptation sets was balanced by flipping the direction of the perturbation (clockwise or counterclockwise) in every successive adaptation set. Participants were allowed to take 5- to 10-minute breaks between paradigms, but not after sets within a paradigm. Each baseline set consisted of 135 null trials, in which participants received veridical feedback on hand position, and 15 pseudo-randomly interspersed clamp trials, in which participants received perfect feedback regardless of movement error. Then, depending on the training paradigm, one of four adaptation sets followed. In the standard training paradigm, the adaptation set consisted of 108 adaptation trials, in which a visuomotor perturbation of 30° was introduced abruptly, and 12 pseudo-randomly interspersed clamp trials (**Figure 2B**). The gradual paradigm contained 108 adaptation trials in the adaptation set, where the visuomotor perturbation of 30° was introduced gradually over the course of the set, increasing linearly each trial. The final 6 trials of the gradual adaptation set were at 30° of visuomotor perturbation. In addition, 12 clamp trials were pseudo-randomly interspersed (**Figure 2C**). The overlearning adaptation set consisted of 324 trials with a visuomotor perturbation of 30° (three times the amount of the standard paradigm) and 36 interspersed clamp trials (**Figure 2D**). The long intertrial interval (ITI) adaptation set included 120 adaptation trials with visuomotor perturbations of 30°, where instead of delay of 2 seconds

between each movement, the delay was increased to 15 seconds (**Figure 2E**). The adaptation set of the long ITI paradigm did not include any clamp trials, thus trial-to-trial forgetting was only dependent on the passage of time. Finally, all adaptation sets were followed by a washout set. The first 12 trials of the washout set consisted of counterperturbation trials, where the direction of the perturbation was flipped from the direction in the adaptation set. Then, 60 clamp trials and 60 null trials followed.

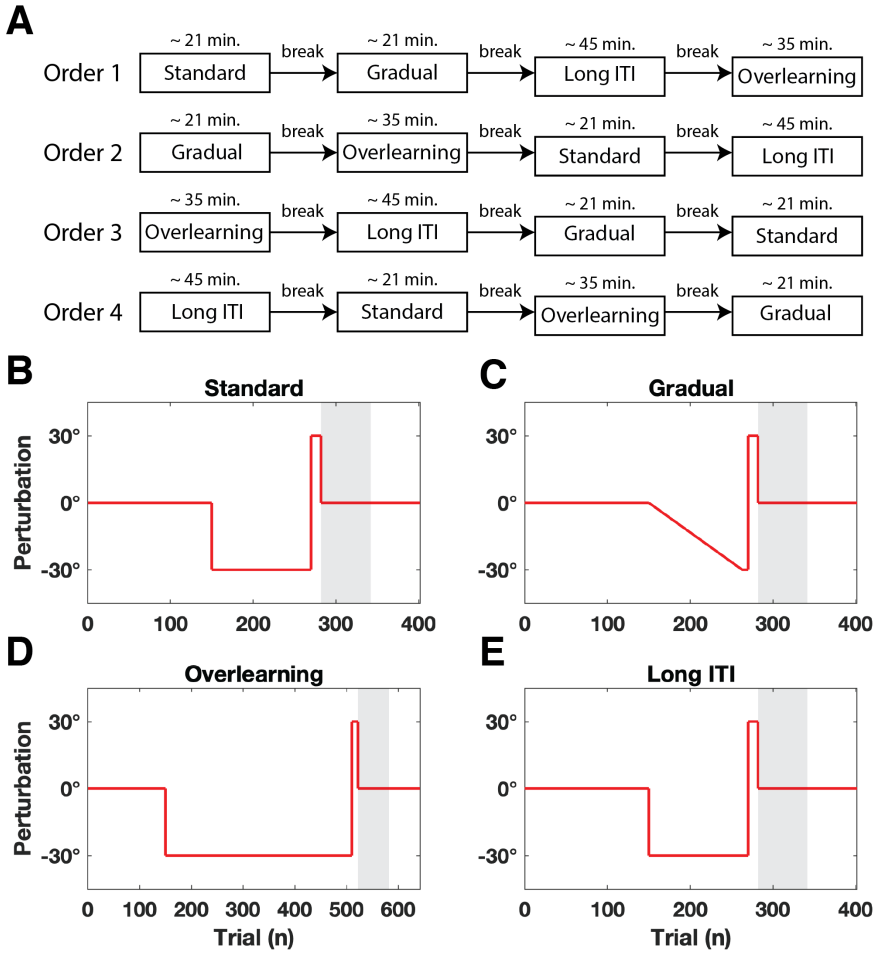

***Figure 2**: A) Overview of the paradigm orders. B–E) Trial structure of the experimental paradigms. Red line indicates the size and direction of the visuomotor perturbation. Direction of the perturbation is pictured here as clockwise for all paradigms, in reality perturbation direction was counterbalanced within participants. Grey area indicates the block of 60 clamp trials in the washout phase. Not pictured are pseudo-randomly interspersed clamp trials during the baseline and adaptation phase.*

2.3 MR imaging

Cerebellar participants and age-matched controls were examined in a 3T combined MRI-PET system (Siemens Healthcare, Erlangen, Germany) with a 16-channel head coil (Siemens

Healthcare) [TR, 2530 ms; TE = 3.26 ms, TI = 1100 ms; flip angle 7 deg; voxel size 0.5 × 0.5 × 1.0 mm^3]. All MR scans were evaluated by an experienced neuroradiologist (SLG). A voxel-based morphometry analysis was applied to the cerebellum of each participant as described previously (Hulst et al., 2015; Taig et al., 2012). The analysis was automated with an in-house program written for MATLAB 9.4 using the SUIT toolbox (version 3.2) (Diedrichsen et al., 2009), implemented in SPM12 (http://www.fil.ion.ucl.ac.uk/spm/software/spm12).

2.4 Analysis of behavioral data

Behavioral data was analyzed in MATLAB 9.4 (Mathworks, Natick, USA). Our primary outcome measure was the reaching direction (in degrees) at the end of the movement (i.e. when participants hit the simulated cushion). The reaching direction was calculated by taking the angle between a straight line from the position of movement onset to the target and a straight line from the position of movement onset to hand position at the end of the movement. Movement onset was defined as the first moment when movement velocity exceeded 5cm/s. Reaching directions were corrected for movement biases by calculating the average reaching direction in each baseline set and subtracting this from the subsequent adaptation and washout sets of a training paradigm. For ease of interpretation, reaching directions were flipped towards the same direction, regardless of perturbation direction, in all figures and analyses. Furthermore, paradigms were reordered to a canonical order for each participant, starting with the standard learning paradigm, then gradual learning, overlearning and finally the long ITI paradigm, regardless of the order the participant encountered the paradigms. Statistical analyses were conducted using Markov Chain Monte Carlo (MCMC) methods in MATLAB and JAGS 4.3.0 (Plummer, 2003). A mixed-design model (ANOVA-like) was used to estimate the difference in reaching directions between factors. Participant group (cerebellar participant or control participant) was included as a between-subject factor.

Movement phase and training paradigm were included as within-subject factors. A random intercept for each participant and phase was included as well. The model ran on four separate chains with an adaptation phase of 5,000 samples and burn-in phase of 25,000 samples, after which we collected 50,000 samples per chain. Each parameter was visually and quantitatively checked to assure proper sampling of the posterior distribution using common MCMC diagnostics (Kruschke, 2010). First, trace plots were visually inspected for chain convergence. Next, the effective sample size (ESS), the potential scale reduction factor (PSRF) and the Monte Carlo Standard Error (MCSE) were calculated for all parameters. The PSRF was close to 1 for each parameter (max: 1.0002), MCSE was close to 0 for each parameter (max: 0.0001), and median ESS was generally large (>> 5000), indicating convergence of the model run. The model code is available as supplementary data on https://github.com/thomashulst/paper-extendedtraining/.

2.5 State-space modeling

A two-state model was fit to the reaching directions of all trials in each individual participant. The equations for the state-space model are given in Equations 1−6:

$$e_t = x_t + p_t \quad \text{(Eq. 1)}$$

$$x^F_{t+1} = A^F x^F_t - B^F e_t + \epsilon_{state} \quad \text{(Eq. 2)}$$

$$x^S_{t+1} = A^S x^S_t - B^S e_t + \epsilon_{state} \quad \text{(Eq. 3)}$$

$$x_t = x^F_t + x^S_t \quad \text{(Eq. 4)}$$

$$y_t = x_t + \epsilon_{output} \quad \text{(Eq. 5)}$$

$$\epsilon_{output} \sim N\left(0, \sigma^2_{\epsilon_o}\right), \epsilon_{state} \sim N(0, \sigma^2_{\epsilon_s}) \quad \text{(Eq. 6)}$$

Where $A^S > A^F$ and $B^S < B^F$.

This state-space model, as posited by Smith and colleagues (Smith et al., 2006), consists of a fast state (x^F_t) and slow state (x^S_t). The fast state learns quickly and forgets quickly, while the slow state learns slowly and forgets slowly. Both states have an independent learning rate (B)

and retention rate (A). Each movement, the fast and slow state are updated based on the error (e) in the previous movement. In visuomotor experiments, the amount of error is given by addition of the actual movement (x_t) and perturbation (p_t). The model has previously been able to predict various behavioral phenomena in reaching adaptation experiments like savings, anterograde interference and spontaneous recovery (Smith et al., 2006).

To estimate the parameters and hidden state variables for a given participant from reaching directions, we implemented a hierarchical model based on Equations $1-6$ in JAGS (**Figure 3**). A hierarchical model improves fits by sharing information across participants. The parameters and state variables were estimated by MCMC methods, separately for each of the four training paradigms (standard, gradual, overlearning and long ITI) and two participant groups (cerebellar participants or control participants). In the hierarchical model, a participants' learning rate (B^S and B^F) and retention rate (A^S and A^F) came from a normal distribution centered around μ with precision τ. The learning and retention rates were sampled in logistic space and then transformed to the range from $0-1$ to more realistically reflect changes in the parameters and provide better sampling behavior. Precision for the states and execution noise came from a very broad gamma distribution ($\mathrm{A} = 10^{-3},\ \mathrm{B} = 10^{-3}$).

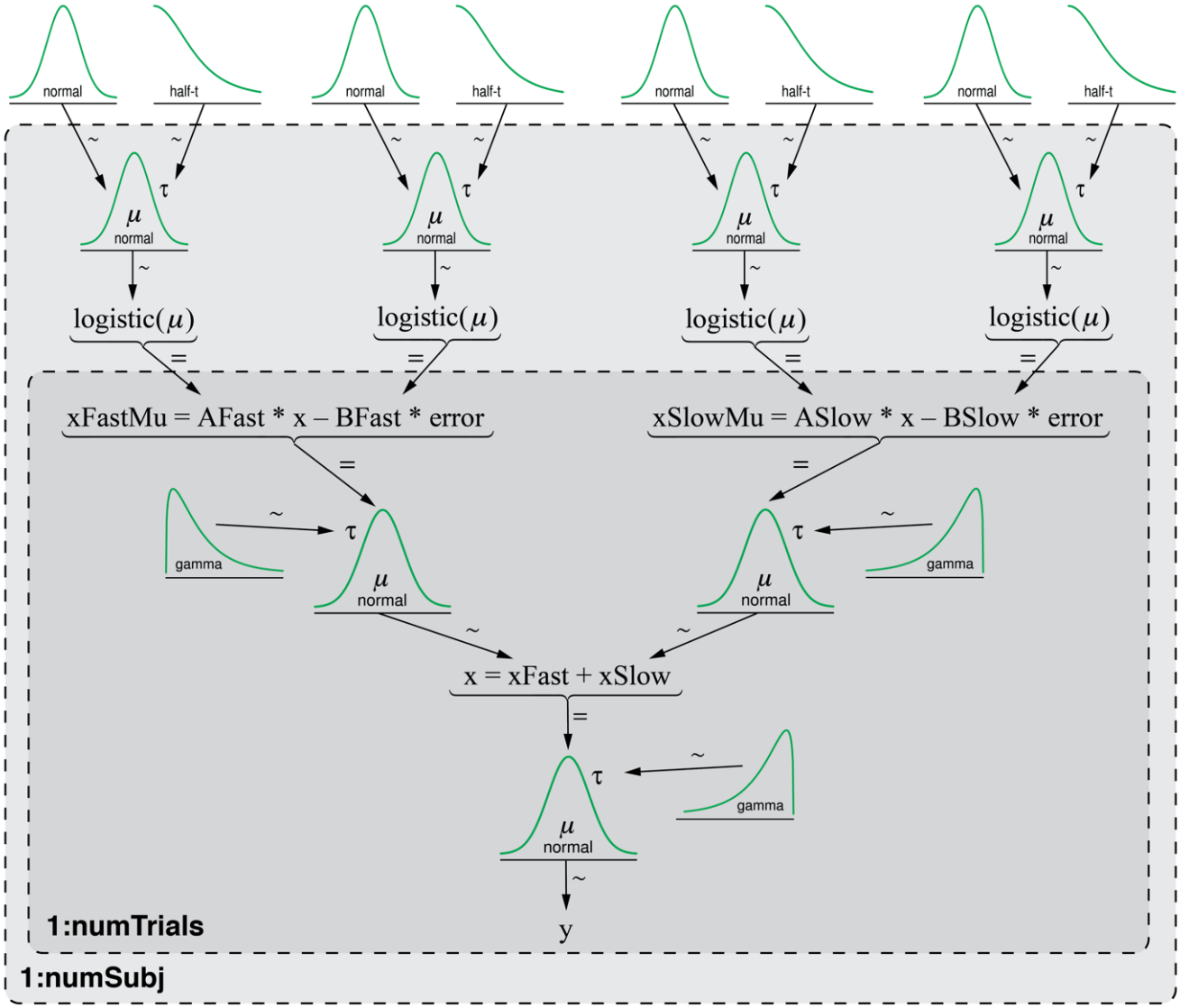

***Figure 3**: Diagram of the hierarchical model implemented in JAGS. The equals sign (=) denotes deterministic relationships, while tildes (~) denote stochastic relationships. The distributions on the white background indicate the hyperpriors. The light grey background indicates the subject loop, while the dark grey background indicates the trial loop.*

Only the shape of the learning- and retention rate distributions was specified (normal in logistic space), the actual priors for each participant were sampled from a hyperprior. The hyperparameter for μ came from an uninformative normal distribution ($M = 0, S = 1000$) and τ from a weakly informed half-t distribution ($M' = 0, S' = 2.5, N = 7$) so each posterior distribution was mainly informed by the data. Reasonable initial values for M and S were estimated by running the model first without hyperpriors and weakly informed priors for the learning and retention rates of a participant (4 chains, adaptation and burn-in of 10,000

samples, 30,000 samples collected). Model runs for the model with hyperparameters started with an adaptation phase of 20,000 samples and burn-in phase of 80,000 samples, after which we collected 250,000 samples on four separate chains. Samples were thinned by a factor of 5 to decrease the memory footprint and autocorrelation of samples. For every parameter we first visually inspected the trace plots for chain convergence. Next, several MCMC diagnostics were calculated: the ESS, PSRF and MCSE. Generally, sampling of the posterior distributions was considered adequate. No large differences in ESS, PSRF and MCSE were found between the paradigms. A small number of parameters had low ESS due to high autocorrelations in specific paradigms, mainly on the participant level, but longer model runs were deemed impractical. The model code is available as supplementary data on https://github.com/thomashulst/paper-extendedtraining/.

3 Results

3.1 Voxel-based morphometry (VBM)

First, the results of the structural MRI data were analyzed using VBM. **Figure 4** displays the difference in gray matter volume per voxel (in t-scores) between healthy participants and cerebellar participants. A resampling procedure (permutation test) was conducted to control the family-wise error rate. The significance threshold was determined to be 3.95, meaning that voxels with an absolute t-score higher than 3.95 were considered significant. No significant positive differences were found, thus the figure displays negative t-scores only. The VBM analysis revealed a pattern of cerebellar degeneration in patients largely consistent with prior work (Hulst et al., 2015). The volume loss was largest in the anterior lobe of the cerebellum and the superior part of the posterior lobe (i.e. lobule VI). Cerebellar degeneration of the anterior cerebellum and lobule VI (i.e. the anterior hand area) are associated with motor learning deficits (Donchin et al., 2012; Rabe et al., 2009). Cerebellar degeneration was less pronounced in the inferior parts of the posterior lobe compared to earlier work (Hulst et al.,

2015), which could be explained by younger cerebellar participants in the current study, with less severe ataxia scores.

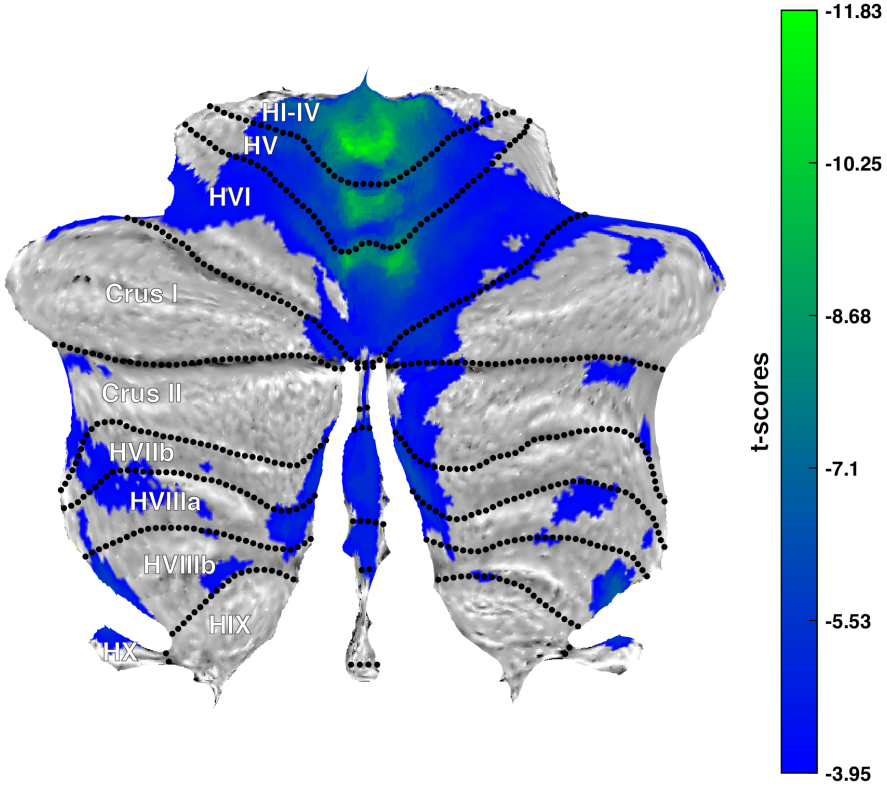

Figure 4*: Flatmap of the cerebellum. Colors indicate the gray matter volume difference per voxel between healthy participants and cerebellar participants in t-scores. Voxels that do not exceed the threshold* (-3.95) *are not colored, low significant t-scores are colored blue, and high significant t-scores are colored green. Flatmap template from Diedrichsen and Zotow, 2015.*

3.2 Average reaching directions

Next, the reaching directions were analyzed. The average reaching directions for each paradigm in control participants and cerebellar participants are plotted in **Figure 5**.

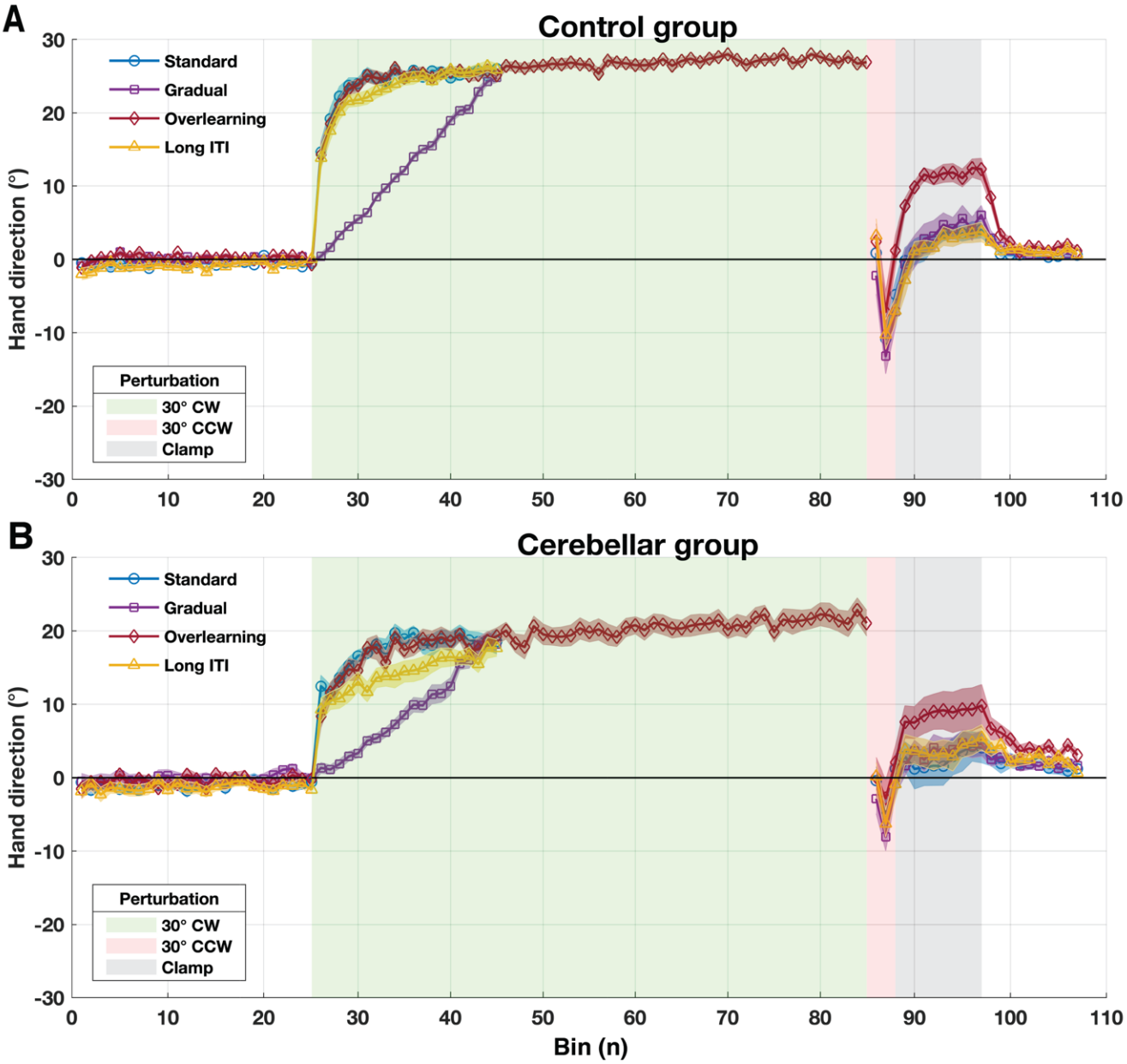

***Figure 5**: Reaching directions of control participants and cerebellar participants, averaged over bins. A) Control participants. B) Cerebellar participants. Trials were binned per 6 trials. Shaded error bars are mean ± SEM.*

As expected, reaching directions of controls participants and cerebellar participants are almost completely straight during the baseline phase in all training paradigms. When movements are perturbed by a visuomotor rotation, control participants learn the perturbation quickly, almost completely counteracting the rotation early in the adaptation set (barring the gradual paradigm). Cerebellar participants adapt much more slowly, counteracting about half of the

rotation compared to healthy controls during the early phases of learning in the standard and overlearning paradigm. Furthermore, the long intertrial interval condition appears to be lagging behind in the amount of early learning compared with the standard and overlearning conditions.

Late in the adaptation set, control participants reach very similar reaching directions in all paradigms. Control participants learn only slightly more after plateauing early in the adaptation set, apart from the obvious difference in the gradual learning condition. Cerebellar participants, on the other hand, learn more after the initial adaptation phase, albeit slowly, which is especially evident in the overlearning paradigm. In general, control participants counteract more of the perturbation both early and late in the adaptation set than cerebellar participants.

After a short phase of counterperturbation trials, both control participants and cerebellar participants exhibit spontaneous recovery in clamp trials immediately following the counterperturbation phase. That is, control participants and cerebellar participants move in the direction of what was previously learned in the absence of a perturbation. The amount of spontaneous recovery is largest in the overlearning paradigm in both groups. While cerebellar participants exhibit higher spontaneous recovery in the overlearning paradigm, the amount of spontaneous recovery is lower than in control participants.

Figure 6 displays individual and mean hand directions as in **Figure 5** but averaged over phases instead of bins. The baseline phase is the average movement direction of all trials in the baseline set, while the early adaptation phase is averaged over the first 30 trials (or 6 bins) of the adaptation set. Late adaptation is averaged over the last 6 trials (last bin) of the adaptation set and the recovery phase is averaged over the clamp trials in the washout set (60 trials or 10 bins). **Figure 6** corroborates the main observations of **Figure 5**. The differences in

mean reaching directions per phase were tested using the mixed-design model described in the methods section. The most important findings are briefly evaluated below.

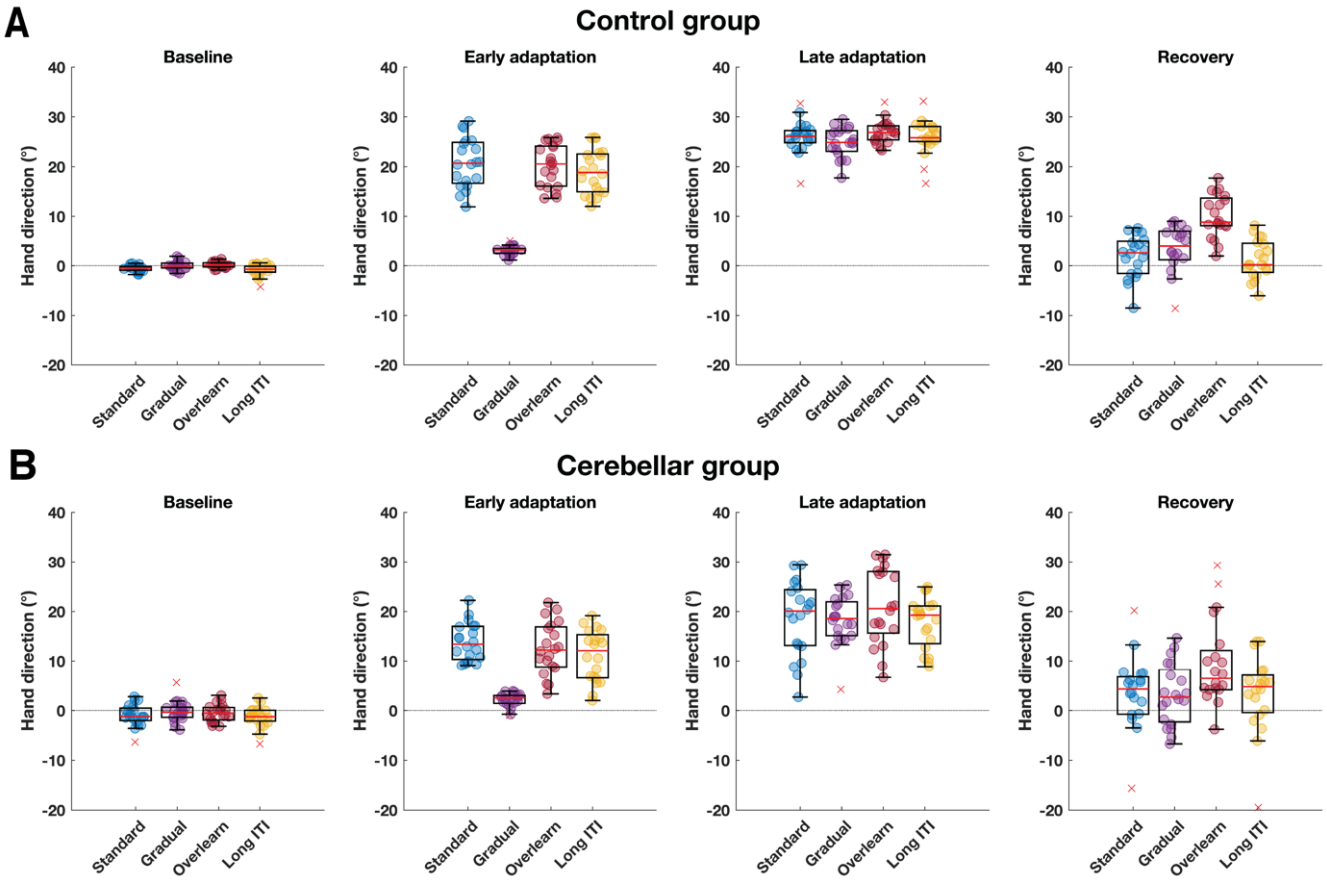

Figure 6*: Boxplots of the reaching directions of control participants and cerebellar participants, averaged over phases. A) Control participants. B) Cerebellar participants. The baseline phase includes all trials in the baseline set. Early adaptation includes the first 30 trials (6 bins) of the adaptation set, while late adaptation is averaged over the last 6 trials (final bin) of the adaptation set. Recovery includes all clamp trials (60 trials) in the washout set. Individual mean reaching directions are indicated with a colored circle. Individual reaching directions more than 1.5 times the interquartile range removed from the first or third quartile are indicated with a red cross.*

Firstly, we tested for differences between the standard, gradual, overlearning and long ITI paradigm in each phase in control participants (**Figure 7**). The MCMC procedure gives us a posterior distribution of credible parameter values, given the data. The parameter of interest in this case was the difference in reaching direction between the standard paradigm and other paradigms. The 95% highest density interval (HDI) contains 95% of the mass of credible parameter values, where each value within the HDI has a higher probability density than any value outside the HDI. When the HDI falls completely within the Region of Practical

Equivalence (ROPE), we accept the null value of the parameter and when the HDI falls completely outside the ROPE, we reject the null value of the parameter. The ROPE was set at $[-3.5°; 3.5°]$. In the baseline phase of control participants, the gradual, overlearning and long ITI paradigms can be regarded as practically equivalent to the standard paradigm, with all credible values of the difference falling within the ROPE. During early learning, the gradual paradigm is obviously different from the standard paradigm, while the overlearning paradigm is practically equivalent. The long ITI paradigm cannot be regarded as equivalent or different from the standard paradigm during early adaptation. Late in learning, both the overlearning and long ITI paradigm are practically equivalent to the standard paradigm, while the HDI of the gradual paradigm falls just outside the ROPE. In the recovery phase, spontaneous recovery is higher in the overlearning paradigm compared to the standard paradigm, while the gradual and long ITI paradigm are practically equivalent.

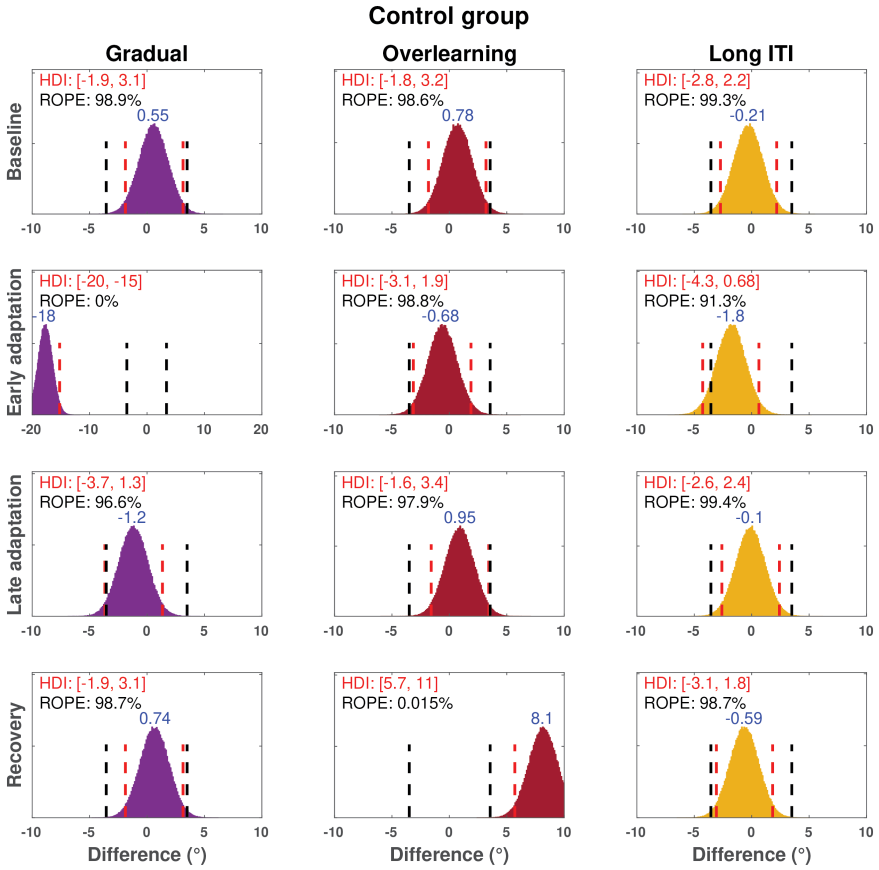

***Figure** 7: Posterior distributions of the difference between the standard paradigm and other paradigms in control participants. The HDI is given in red text and red bars, the ROPE in black bars, and the percentage of the HDI within the ROPE in black text. The mode of the posterior distribution is given by blue text centered around the mode.*

Secondly, we tested for differences between paradigms in the cerebellar group (**Figure 8**). In the cerebellar group, similar differences and equivalencies between paradigms were established. That is, the baseline paradigms are practically equivalent, while the gradual paradigm is obviously different from the standard paradigm during the early adaptation phase. The overlearning and long ITI paradigm HDI's fall just outside the ROPE during early learning, failing to establish equivalency. Late in adaptation, the gradual paradigm and long ITI paradigm are practically equivalent to the standard learning paradigm, while no decision criterion is met for the overlearning paradigm late in adaptation. Spontaneous recovery in the gradual paradigm and long ITI paradigm is practically equivalent to the standard paradigm. Credible values for the overlearning paradigm are higher than the standard paradigm, but the HDI and ROPE overlap slightly (5.46% of credible values fall within the ROPE). In other words, while the credible values for our parameter of interest are highly suggestive for a difference between the standard paradigm and overlearning paradigm in the recovery phase in cerebellar participants, the null value cannot be fully rejected given a ROPE of $[-3.5°; 3.5°]$.

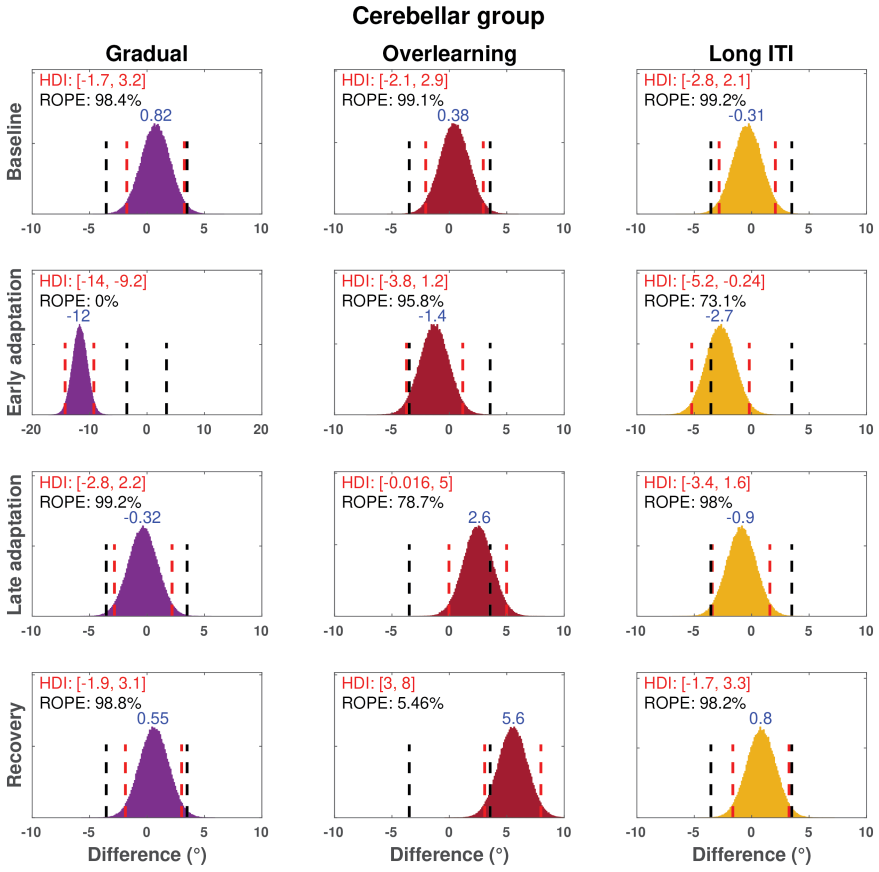

Figure 8*: Posterior distributions of the difference between the standard paradigm and other paradigms in cerebellar participants. The HDI is given in red text and red bars, the ROPE in black bars, and the percentage of the HDI within the ROPE in black text. The mode of the posterior distribution is given by blue text centered around the mode.*

Finally, we tested for differences between control participants and cerebellar participants (**Figure 9**). The baseline phase is practically equivalent for all paradigms between control participants and cerebellar participants. Early learning is much higher in control participants in all paradigms except the gradual paradigm, for which no decision criterion is met. The late adaptation phase is suggestive of more learning in control participants, but all HDI's overlap the ROPE. The recovery phase is suggestive of similar spontaneous recovery between control participants and cerebellar participants, but too much of the HDI falls outside the ROPE in all paradigms to establish equivalency.

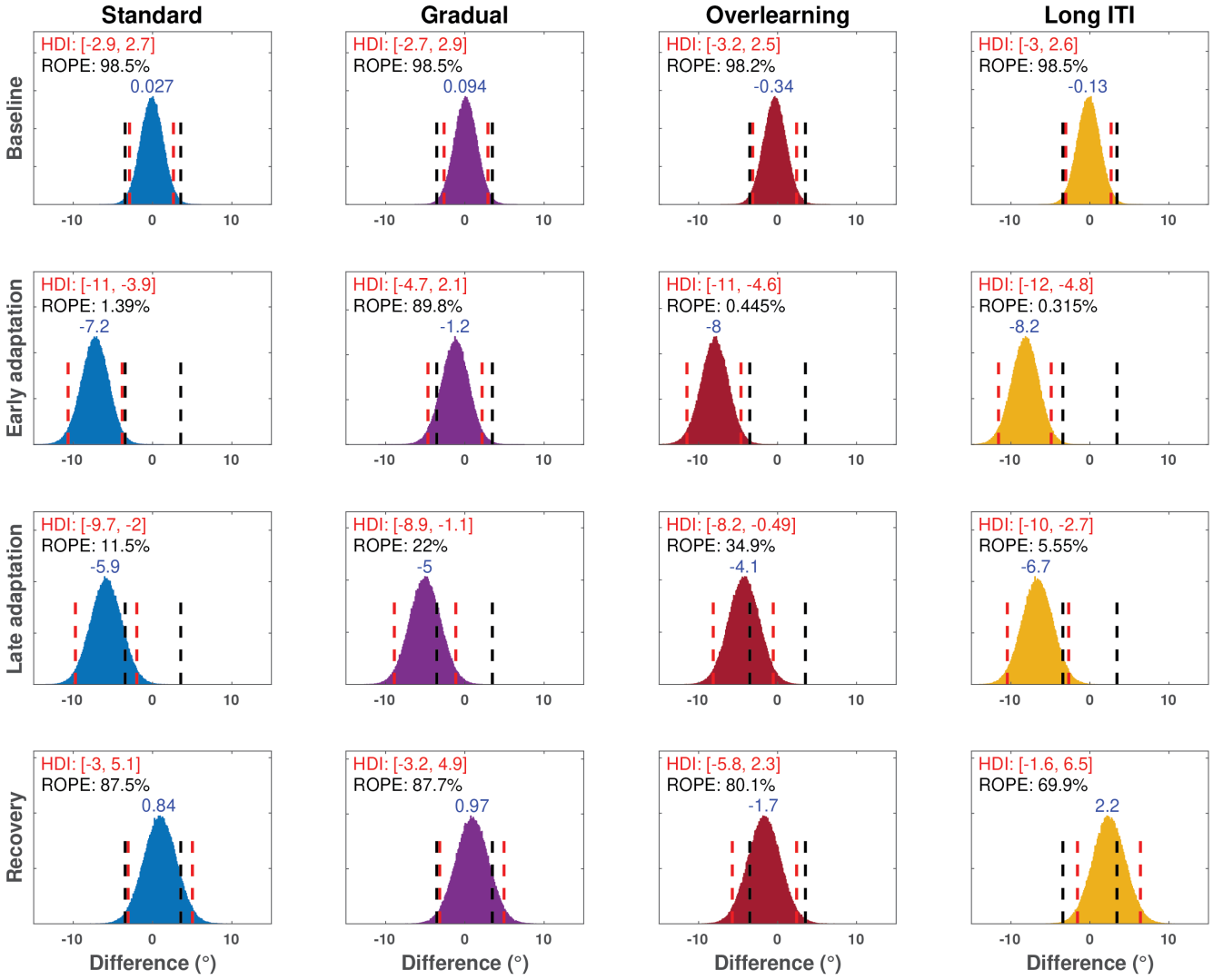

***Figure 9**: Posterior distributions of the difference between control participants and cerebellar participants (cerebellar participants – control participants). The HDI is given in red text and red bars, the ROPE in black bars, and the percentage of the HDI within the ROPE in black text. The mode of the posterior distribution is given by blue text centered around the mode of the posterior distribution.*

To sum up, behaviorally, the most salient difference in control participants exists between the amount of spontaneous recovery in the standard paradigm versus the overlearning paradigm, i.e. there is more spontaneous recovery after overlearning than standard learning. Similarly, the difference between the overlearning paradigm and the standard paradigm in cerebellar participants is highly suggestive for more spontaneous recovery after overlearning as well, though the difference is smaller than in control participants. We hypothesized that the additional amount of spontaneous recovery in both groups could either be due to prolonged

406 activation of the slow learning system, thereby increasing buildup of the slow state, or due to
407 changes in the learning and retention parameters themselves. These hypotheses will be
408 explored in the next section.

409 *3.3 Model results*

410 Since behavioral differences between the paradigms were mainly evident in overlearning
411 versus standard learning, the following section focusses on comparing these paradigms. The
412 model results for the other paradigms can be found as supplementary data (**Supplementary**
413 **data: Table 2-1 and Figures 10-1 and 10-2**).

414 To assess whether the estimated learning rate and retention rate of individual participants
415 changed between paradigms, we plotted the credible values of A and B parameters of each
416 participant in the standard paradigm versus the overlearning paradigm (**Figure 10**).

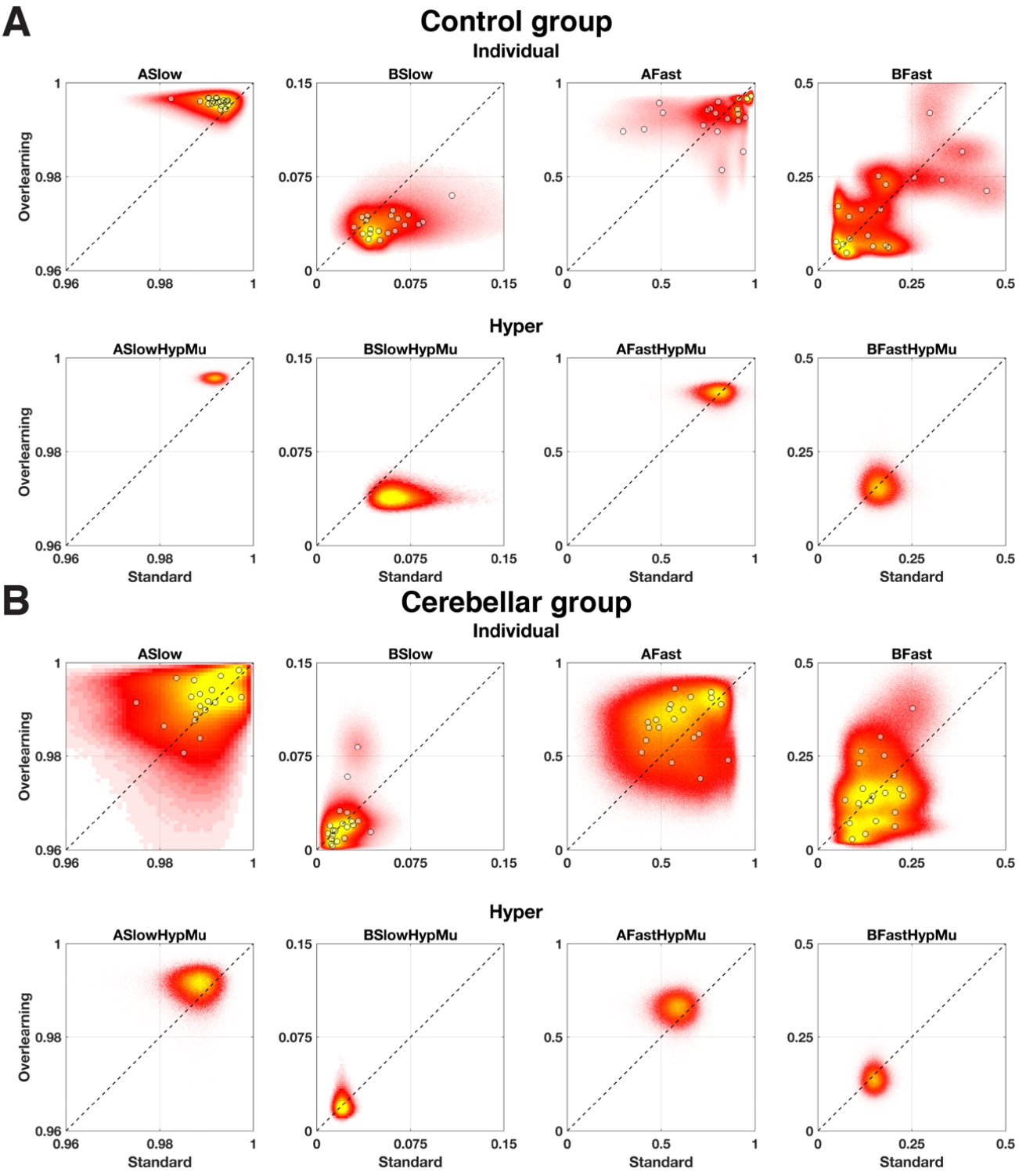

***Figure 10**: Bivariate histograms of the credible parameter values of individual participants and hyperparameters in the standard versus overlearning paradigm. All samples of the overlearning paradigm (y-axis) were distributed over 500 bins and plotted as a function of the standard paradigm (x-axis). Sample counts range from relatively few samples from the posterior distribution (red) to many samples from the posterior distribution (yellow). The black dashed line indicates equality between paradigms. Circles indicate the modal parameter value of individual participants. A) Control participants B) Cerebellar participants.*

Two changes in the parameters between the paradigms were discernable in control participants (**Figure 10A**). Most notably, the retention rate of the slow state (A_{Slow}) was shifted towards higher values in the overlearning paradigm in control participants (i.e. more retention of the slow system). Furthermore, the learning rate of the slow state (B_{Slow}) was shifted towards lower values in the overlearning paradigm in control participants (i.e. slower learning of the slow system). Thus, the slow learning system is less sensitive to error as a result of extended training. The learning and retention rates of the fast system (A_{Fast} and B_{Fast}) appeared equivalent between the paradigms in control participants. The shifts of A_{Slow} and B_{Slow} were also reflected in the posterior distributions of the hyperparameters in control participants (second row, **Figure 10A**).

In patients, changes in parameters between the paradigms were less discernable (**Figure 10B**). Qualitatively, it appears that cerebellar participants have a slightly higher retention rate of the slow system (A_{Slow}) in the overlearning paradigm, like controls participants, but not a lower adaptation rate of the slow system (B_{Slow}). Furthermore, credible values of A_{Fast} appeared to shift towards slightly higher values in the overlearning paradigm. The modal values and HDI's of the hyperparameters of both control participants and cerebellar participants are printed in **Table 2**. Comparing the hyperparameters of control participants to cerebellar participants, we found that the values of A_{Slow}, B_{Slow}, and A_{Fast} are generally higher in control participants in both paradigms, while B_{Fast} is equivalent between participant groups. Bivariate histograms of control participants versus cerebellar participants which further illustrate these observations are found in the extended materials (**Supplementary data: Figure 10-3**).

Table 2

Mode and HDI's of hyperparameters in two-state model

Control participants				
	Normal		**Overlearning**	
Parameter	**Mode**	**HDI**	**Mode**	**HDI**
ASlowHypMu	0.992	0.989 – 0.994	0.996	0.994 – 0.997

BSlowHypMu	0.057	0.040 – 0.103	0.039	0.029 – 0.052
AFastHypMu	0.81	0.664 – 0.903	0.82	0.750 – 0.868
BFastHypMu	0.16	0.113 – 0.221	0.154	0.106 – 0.214
Cerebellar participants				
	Normal		**Overlearning**	
Parameters	**Mode**	**HDI**	**Mode**	**HDI**
ASlowHypMu	0.988	0.982 – 0.994	0.992	0.986 – 0.995
BSlowHypMu	0.02	0.013 – 0.029	0.021	0.009 – 0.040
AFastHypMu	0.588	0.454 – 0.695	0.669	0.550 – 0.757
BFastHypMu	0.15	0.115 – 0.188	0.134	0.094 – 0.185

***Table 2**: Mode and HDI of credible parameter values in control participants and cerebellar participants. HDI is the 95% highest density interval. Parameter names correspond with nodes in JAGS model code.*

3.4 Posterior predictive plots

To assess how the differences in the learning and retention rate between training paradigms affect motor output (y_t) and the states (x_t^F and x_t^S), posterior predictive plots were generated from multiple random draws (n = 10.000) of the posterior distributions of each participant (**Figure 11**). The model output ($\hat{y}_t$) generated from the posterior distributions generally fits behavior, with some notable exceptions. We will first discuss how shifts in parameters between paradigms are reflected in the posterior predictive plots. In the next section (Section 3.5), we will assess the ways in which the model output does not fit the behavioral data, since the amount of early learning and spontaneous recovery is generally underestimated, especially in the overlearning paradigm.

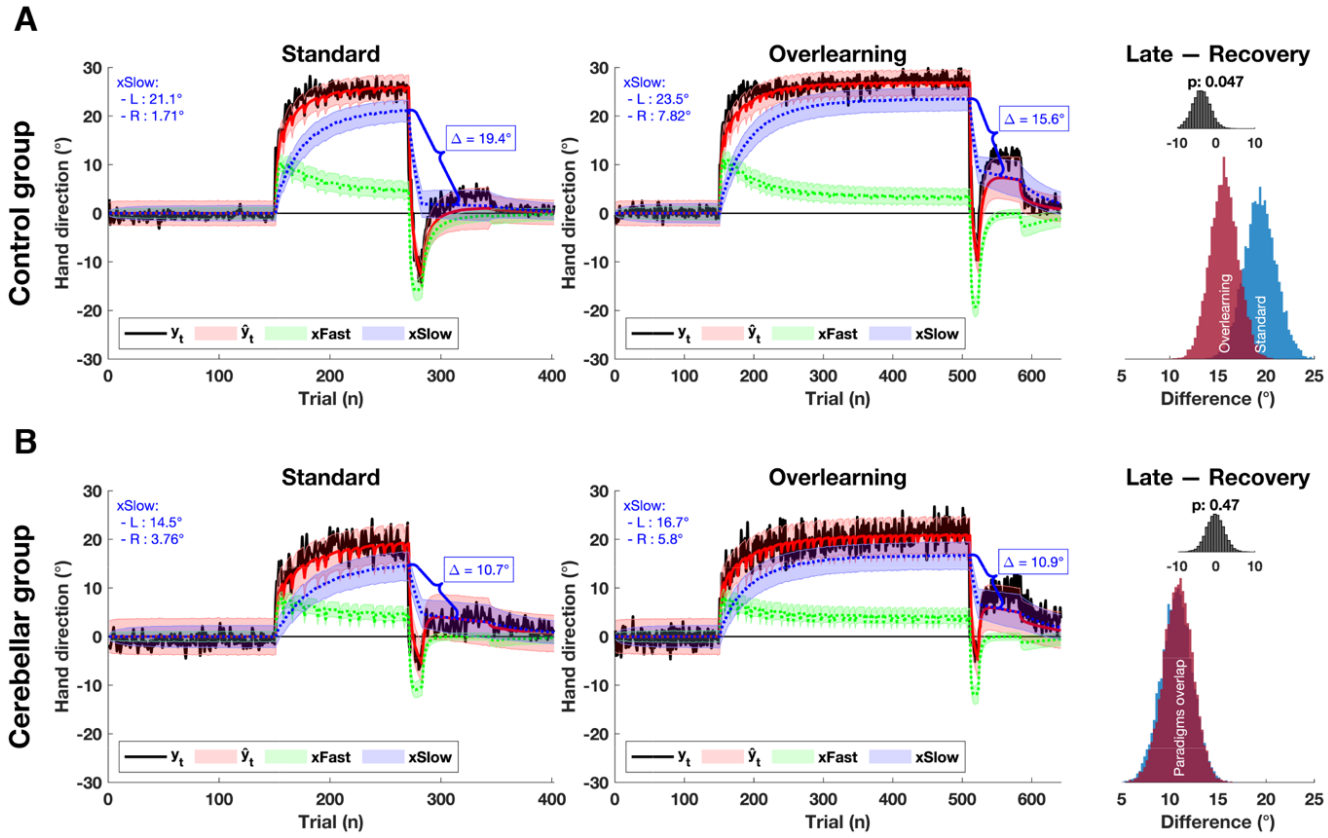

457

458 ***Figure 11***: *Posterior predictive plots of standard and overlearning paradigm. A) Control participants. B)*
459 *Cerebellar participants. In the left and middle panels, the average behavior (y_t) is displayed with a solid black*
460 *line for the standard paradigm an overlearning paradigm respectively. The average model output ($\hat{y}_t$) is*
461 *displayed with a solid red line, the average fast state (x_t^F) with a dotted green line, and the average slow state*
462 *(x_t^S) with a dotted blue line. The shaded errorbars indicate the variability around the average posterior*
463 *predictive (2.5^{th} percentile – 97.5^{th} percentile of simulated data). In the top left corner of the left and middle*
464 *panels, the average value of the slow state late in adaptation (L: the last 6 trials of the adaptation set) and the*
465 *recovery phase (R: all 60 clamp trials in the washout set) is printed. Δ indicates the difference between the*
466 *average slow state late in adaptation and the recovery phase ($L - R$). The distribution of Δ for all 10.000 draws*
467 *is plotted in the rightmost panel. The blue histogram indicates Δ for the standard paradigm, while the red*
468 *histogram indicates Δ for the overlearning paradigm. The inset histogram is the distribution of differences*
469 *between Δ of the standard and overlearning paradigm (overlearning – standard) and displays the proportion (p)*
470 *of draws with a difference larger than 0.*

471 In the standard and overlearning paradigm in both groups, the model predicts large amounts
472 of learning early in the adaptation set, driven by a quick rise of the fast state and a gradual rise
473 of the slow state (**Figure 11**). Nearing the end of the adaptation set in both paradigms and
474 groups, the model output is dominated by the slow state. The fast state quickly unlearns the
475 perturbation during counterperturbation trials in both groups and paradigms, while the slow
476 state is more resistant to the flip in perturbation direction. The recovery phase is dominated by

the slow state, but as mentioned above and further explored in Section 3.5, the model generally underestimates the amount of spontaneous recovery.

In control participants, the slow state reaches similar levels of adaptation in both paradigms, about 21.1 degrees and 23.5 degrees for standard learning and overlearning respectively (**Figure 11A**). In the recovery phase of the standard paradigm the slow state is reduced to approximately 1.7 degrees, while the slow state in the overlearning paradigm retains approximately 7.8 degrees of what was learned. Thus, the difference between the slow state late in adaptation and the recovery phase is much larger in the standard paradigm than the overlearning paradigm (19.4 degrees versus 15.6 degrees respectively). This indicates that, in control participants, additional buildup of the slow state over the longer adaptation set is not the driving force behind additional spontaneous recovery as hypothesized, rather the motor memory has become more resilient, possibly due to the changes in the underlying parameters between paradigms.

Contrastingly, in cerebellar participants, the difference between the slow state at the end of adaptation and the recovery phase is practically equivalent between the standard and overlearning paradigm, 10.7 degrees versus 10.9 degrees respectively (**Figure 11B**). Thus, while behaviorally there is more spontaneous recovery in the overlearning paradigm in cerebellar participants, this can largely be attributed by extended buildup of the slow state. By generating posterior predictive plots from the learning and retention parameters of the standard paradigm applied to the experimental structure of the overlearning paradigm (and vice versa), we could assess how much of the amount of slow learning in the recovery phase was explained by differences in parameters between the paradigms (**Figure 12**).

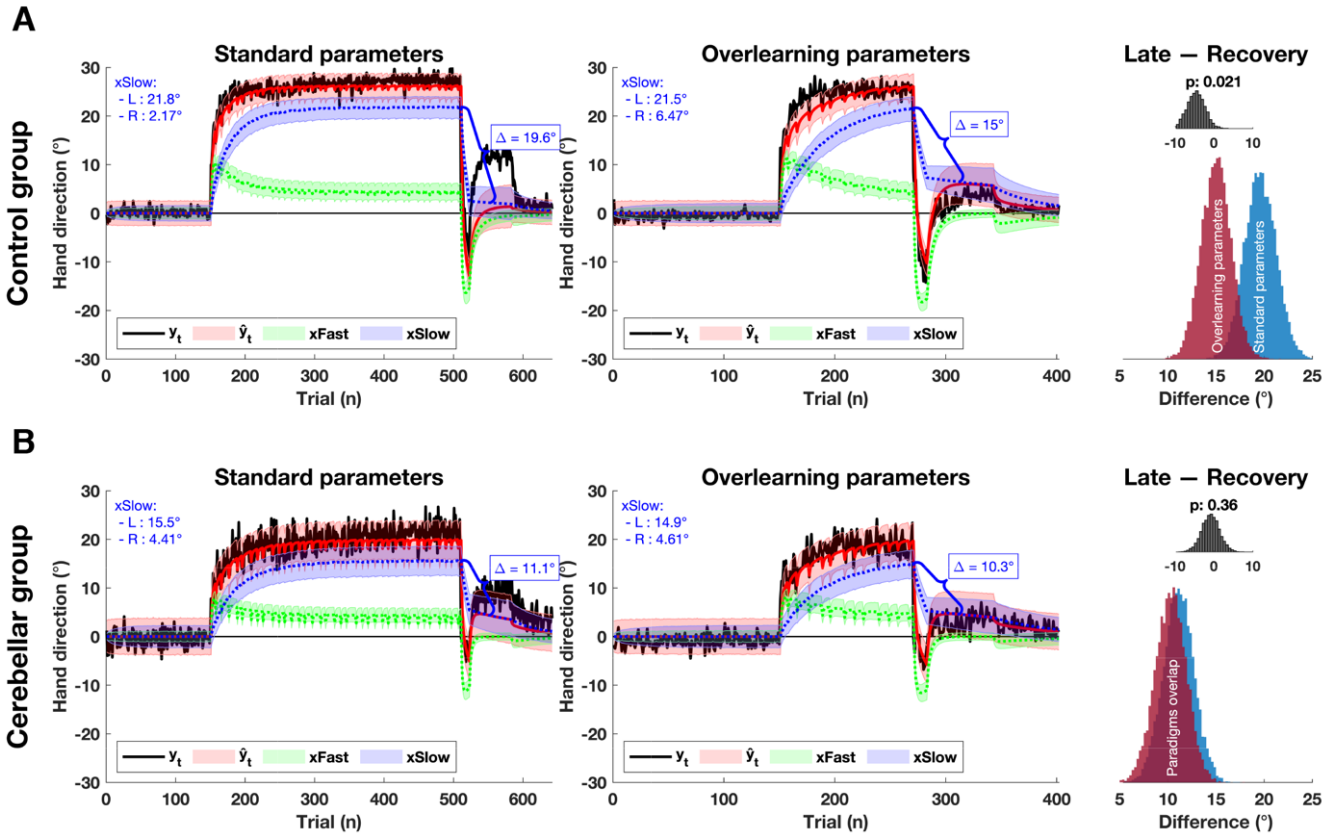

***Figure 12**: Posterior predictive plots of the standard and overlearning paradigm generated from parameter sets of the other paradigm. A) Control participants. B) Cerebellar participants. In the left and middle panels, the average behavior (y_t) is displayed with a solid black line for the overlearning and standard paradigm respectively. The average model output ($\hat{y}_t$) is displayed with a solid red line, the average fast state (x_t^F) with a dotted green line, and the average slow state (x_t^S) with a dotted blue line. The shaded errorbars indicate the variability around the average posterior predictive (2.5th percentile – 97.5th percentile of simulated data). In the top left corner of the left and middle panels, the average value of the slow state late in adaptation (L: the last 6 trials of the adaptation set) and the recovery phase (R: all 60 clamp trials in the washout set) is printed. Δ indicates the difference between the average slow state late in adaptation and the recovery phase (L − R). The distribution of Δ for all 10.000 draws is plotted in the rightmost panel. The blue histogram indicates Δ for standard parameters in the overlearning structure, while the red histogram indicates Δ for overlearning parameters in the standard structure. The inset histogram is the distribution of differences between Δ of the standard parameters and overlearning parameters (overlearning – standard) and displays the proportion (p) of draws with a difference larger than 0.*

Notably, using incongruent parameter sets, the slow state reaches similar levels at the end of adaptation in the standard and overlearning experimental structure, both in control participants (**Figure 12A**) and cerebellar participants (**Figure 12B**). However, motor memory is only more resilient in the experimental structure with overlearning parameters in control participants, but not in cerebellar participants. This observation further establishes the idea that a shift in model rates between paradigms is what drives most of the additional

spontaneous recovery during overlearning, and that cerebellar participants have reduced motor memory resilience since their parameters change less as a function of overlearning. Finally, we wanted to assess whether the additional memory resilience after overlearning in control participants was driven largely by the changes in the retention parameter of the slow system (A_{Slow}) or by changes in the learning parameter of the slow system (B_{Slow}). Therefore, posterior predictive plots were generated from the original posterior distributions, but either A_{Slow} or B_{Slow} was drawn from the posterior distribution of the other paradigm (**Figure 13**). Posterior predictive plots are only shown for control participants, plots for cerebellar participants can be found in the extended materials (**Supplementary data: Figure 13-1**).

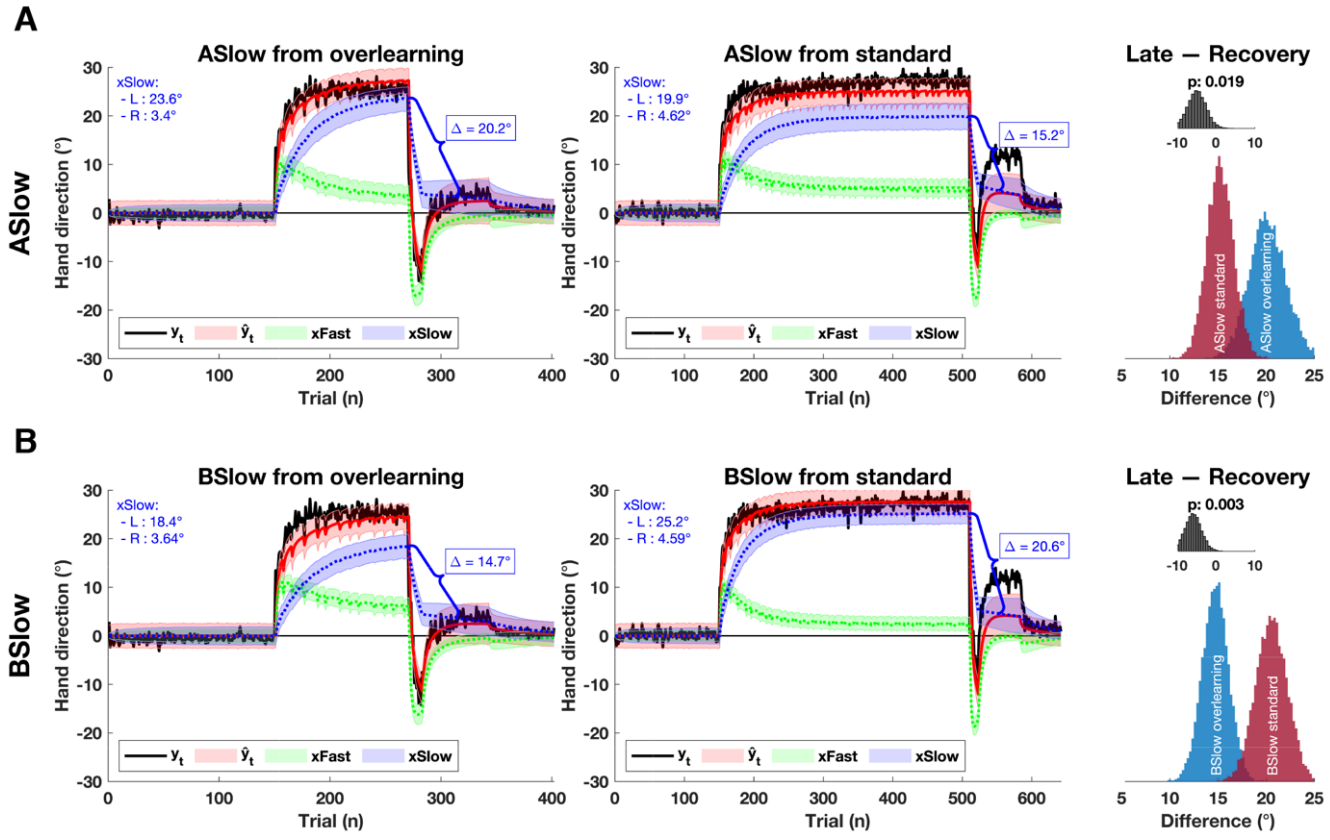

***Figure 13**: Posterior predictive plots of the standard and overlearning paradigm, but with ASlow or BSlow from the other paradigm. Only the posterior predictive plots of control participants are shown. A) ASlow drawn from the other paradigm. B) BSlow drawn from the other paradigm. In the left and middle panels, the average behavior (y_t) is displayed with a solid black line for the standard paradigm an overlearning paradigm respectively. The average model output ($\hat{y}_t$) is displayed with a solid red line, the average fast state (x_t^F) with a dotted green line, and the average slow state (x_t^S) with a dotted blue line. The shaded errorbars indicate the variability around the average posterior predictive (2.5th percentile – 97.5th percentile of simulated data). In the top left corner of the left and middle panels, the average value of the slow state late in adaptation (L: the last 6*

trials of the adaptation set) and the recovery phase (R: all 60 clamp trials in the washout set) is printed. Δ indicates the difference between the average slow state late in adaptation and the recovery phase (L − R). The distribution of Δ for all 10.000 draws is plotted in the rightmost panel. The blue histogram indicates Δ for the standard paradigm with one parameter from overlearning, while the red histogram indicates Δ for the overlearning paradigm with one parameter from standard learning. The inset histogram is the distribution of differences between Δ of the standard and overlearning paradigm. The paradigm with the larger amount of spontaneous recovery was subtracted from the smaller amount. The proportion (p) of draws with a difference larger than 0 is printed on top.

For the posterior predictive plots with A_{Slow} drawn from the other paradigm, the general pattern of learning and retention is similar to the original posterior predictive plots (**Figure 11A**). There is slightly more buildup of the slow state during adaptation in the standard paradigm with A_{Slow} drawn from the overlearning posterior (cf. **Figure 11A**), which suggests that A_{Slow} determines the extent of the slow state at the end of learning. However, the motor memory is still less resilient than the overlearning paradigm, given the relatively large difference between the slow state late in adaptation and the recovery phase (20.2 degrees, **Figure 13A**). In the overlearning paradigm, with A_{Slow} drawn from the standard posterior, we see slightly less buildup of the slow state during adaptation (cf. **Figure 11A**), but the motor memory remains relatively resilient (a difference of 15.2 degrees between late adaptation and the recovery phase, **Figure 13A**).

However, when B_{Slow} is drawn from the posterior of the other paradigm, we see a complete reversal of the pattern of memory resilience (**Figure 13B**). Now, the paradigm with the most resilient motor memory is the standard paradigm, instead of the overlearning paradigm. During the overlearning paradigm (middle panel, **Figure 13B**), the slow state reaches higher levels during adaptation than the slow state in the original posterior predictive plot of the overlearning paradigm (middle panel, **Figure 11A**). However, the difference of the slow state late in adaptation and the recovery phase is much larger than the posterior predictive with congruent parameters, revealing that motor memory resilience is mainly driven by a reduction in the learning rate of the slow system (B_{Slow}). This also illustrates why cerebellar participants exhibit less spontaneous recovery than control participants. Since B_{Slow} in cerebellar

participants remains relatively constant between the standard paradigm and overlearning paradigm (**Figure 10B**), motor memory resilience of cerebellar participants is not increased by overlearning.

3.5 Exploring the lack of fit

As briefly alluded to in the prior section, the amount of early learning and spontaneous recovery is underestimated compared to the actual behavioral response, especially in the overlearning paradigm. We hypothesized that this could be due to the fact that the model identifies a fixed set of parameters for all trials, while in reality learning and retention rates change dynamically in response to task demands. As the learning and retention rates are considered fixed in the model, any changes due to developing task demands might be 'averaged out'. That is, because the parameters are considered constant, the model has a hard time accounting for both the large amount of quick early learning in the adaptation set, as well as the increase in memory resilience due to overlearning.

This hypothesis was explored by splitting the behavioral data in half and performing a model run for each part separately. The first split of behavioral data contained the trials of the baseline set and the early learning of the adaptation set, while the second split consisted of the trials late in adaptation, the counterperturbation trials, the recovery phase, and the washout phase. Thus, practically, an independent set of parameters was identified for each split of a paradigm.

First, we assessed whether the parameters actually changed between the two splits of behavioral data. For this purpose, the learning and retention rate of the first split were plotted versus the rates of the second split (**Figure 14**).

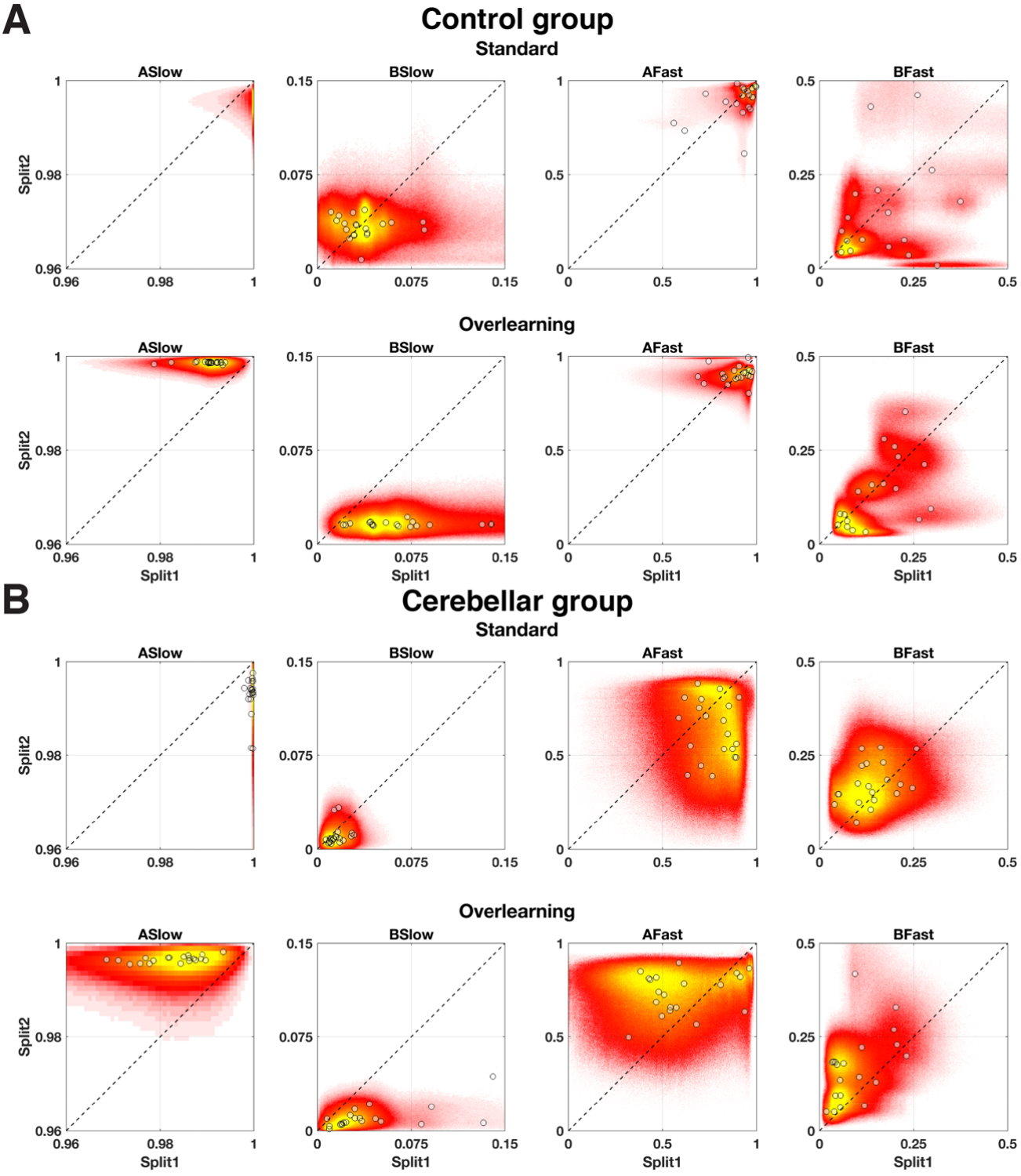

Figure 14: *Bivariate histograms of the credible parameter values of individual participants in the first split (Split1) versus the second split (Split 2). A) Control participants. B) Cerebellar participants. Both the standard learning paradigm and overlearning paradigm are pictured. All samples of the second split (y-axis) were distributed over 500 bins and plotted as a function of the first split (x-axis). Sample counts range from relatively few samples from the posterior distribution (red) to many samples from the posterior distribution (yellow). The black dashed line indicates equality between paradigms. Circles indicate the modal parameter value of individual participants.*

This suggested that the parameters of control participants are relatively stable in the standard learning paradigm, with the exception of A_{Slow}. A_{Slow} is close to 1 during the first split in all participants, likely since adaptation has not plateaued in the early trials of the standard learning paradigm. In contrast, the learning and retention rates of control participants in the overlearning paradigm change quite dramatically between splits. Specifically, the parameters of the slow state (A_{Slow} and B_{Slow}) are shifted in the second half of the paradigm versus the first half. A_{Slow} is generally higher in the second split, while B_{Slow} is generally lower in the second split.

In cerebellar participants, the shifts in parameters between the splits in the standard paradigm are mostly equivalent to control participants, though B_{Slow} also appears to be slightly lower in the second split than the first split in the standard paradigm. In the overlearning paradigm, however, not only are there similar shifts to the parameters of the slow state as seen in control participants (A_{Slow} and B_{Slow}), there is also a shift in the parameters of the fast state between splits. Namely, both A_{Fast} and B_{Fast} are higher in the second split than the first split.

To explore whether 'averaging out' the changes in parameters was actually the reason of the poor fit early in the adaptation set and recovery phase, multiple random draws (n = 10.000) were taken from the posteriors of each participant in both splits of the model data. Then, posterior predictive plots were generated from these draws and fitted to the respective split of behavioral data (**Figure 15**). The earlier observation that motor memory becomes more resilient with overlearning in control participants, but not cerebellar participants, also holds in the split model posterior predictive plots. The additional spontaneous recovery in cerebellar participants is fully explained by additional buildup of the slow state during adaptation, and not increased memory resilience. Importantly, in both paradigms and participant groups, the output of the split models clearly fits the behavioral data better than the unsplit model runs. Both the amount of early learning and the spontaneous recovery is estimated more accurately

in the split model than the unsplit model, further indicating that model parameters change dynamically in response to task demands, rather than being constant across all movements.

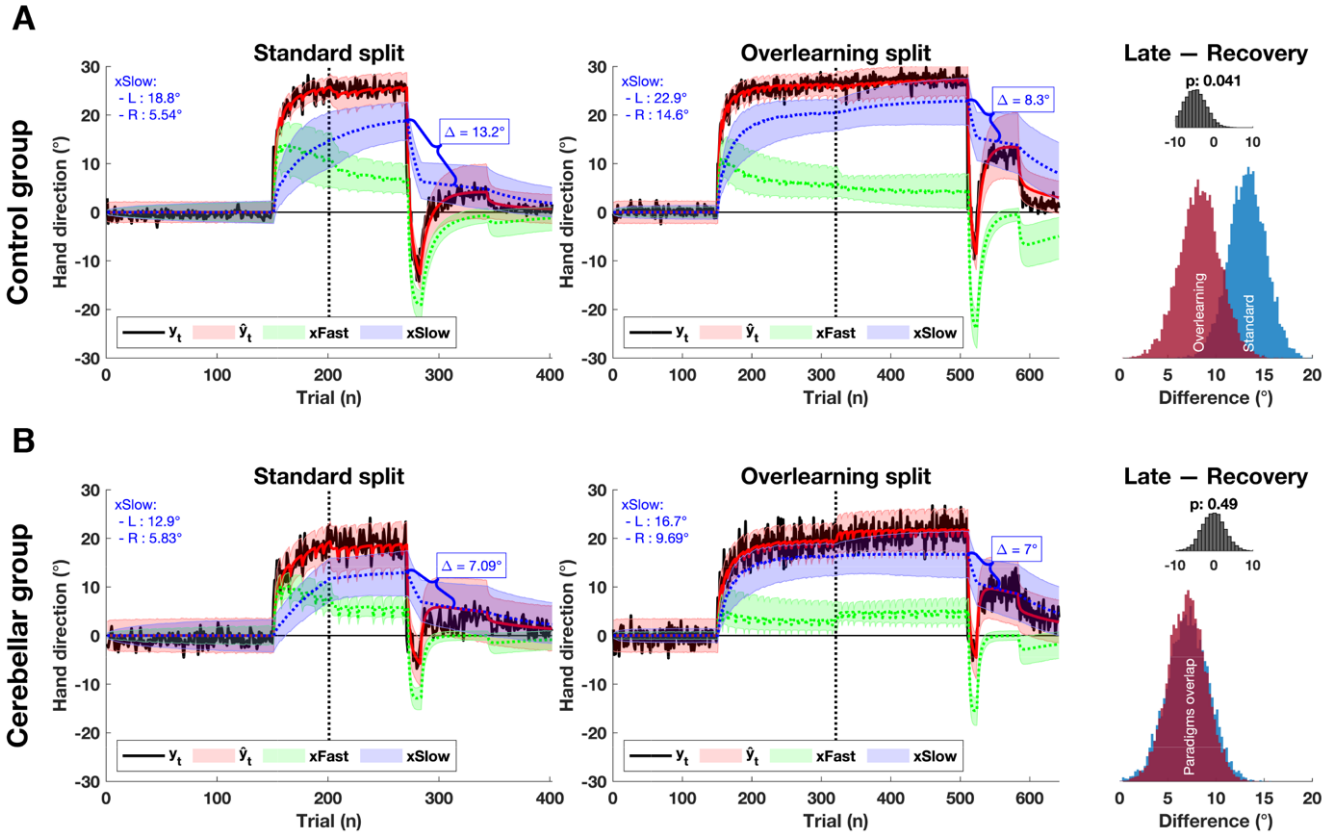

Figure 15: *Posterior predictive plots of the standard and overlearning paradigm using split model parameters. A) Control participants. B) Cerebellar participants. In the left and middle panels, the average behavior (y_t) is displayed with a solid black line for the overlearning and standard paradigm respectively. The average model output ($\hat{y}_t$) is displayed with a solid red line, the average fast state (x_t^F) with a dotted green line, and the average slow state (x_t^S) with a dotted blue line. The shaded errorbars indicate the variability around the average posterior predictive (2.5^{th} percentile – 97.5^{th} percentile of simulated data). In the top left corner of the left and middle panels, the average value of the slow state late in adaptation (L: the last 6 trials of the adaptation set) and the recovery phase (R: all 60 clamp trials in the washout set) is printed. Δ indicates the difference between the average slow state late in adaptation and the recovery phase (L − R). The distribution of Δ for all 10.000 draws is plotted in the rightmost panel. The blue histogram indicates Δ for the standard paradigm, while the red histogram indicates Δ for the overlearning paradigm. The inset histogram is the distribution of differences between Δ of the standard and overlearning paradigm (overlearning − standard) and displays the proportion (p) of draws with a difference larger than 0.*

638 **4 Discussion**

639 In the following paragraphs we will discuss our most important observations in more detail,
640 the possible implications for cerebellar therapy, and address limitations of the present study.

641 *4.1 What drives memory resilience?*

642 Essentially, in control participants, extended training reduces sensitivity to new movement
643 errors. Error sensitivity depends on several factors, like the size of the movement error
644 (Marko et al., 2012), planning/execution noise (van der Vliet et al., 2018), the history of
645 movement errors (Herzfeld et al., 2014) and the uncertainty of movement errors (Wei, 2010).
646 We suggest that the reduction in error sensitivity in the overlearning paradigm is the result of
647 reduced state estimation uncertainty (Kording et al., 2007). Assuming motor learning is a
648 process of optimally combining feedforward estimates and sensory feedback, the motor
649 learning system should adapt slower to new movement errors given reduced state estimation
650 uncertainty. Thus, after extended training, counterperturbation trials are slower to washout the
651 slow state, resulting in increased levels of spontaneous recovery in control participants.
652 The reduction in error sensitivity appears to contrast with earlier work, which suggests that
653 error sensitivity increases in response to more consistent error environments (Herzfeld et al.,
654 2014). Herzfeld et al. found that participants learned more from movement errors when an
655 error environment was likely to persist, while learning from movement errors was suppressed
656 in rapidly switching environments. However, in that study, error sensitivity was measured on
657 a trial-by-trial basis, which likely captured error sensitivity of the fast process to a much
658 greater extent than the slow process. Furthermore, the authors did not consider how extended
659 exposure to a particular environment affected the resilience of that environment. Therefore,
660 our findings are likely congruent with these earlier results, as increasing error sensitivity of
661 the fast process and reducing error sensitivity of the slow process might work in parallel.

662 *4.2 Why is motor memory resilience attenuated in cerebellar participants?*

Some researchers have suggested that the properties of the fast learning system are associated with the cerebellar cortex, while the properties of the slow system are associated with the deep cerebellar nuclei (DCN) (Antonietti et al., 2017; Casellato et al., 2015; Medina et al., 2001). We observed degeneration of the anterior hand area of the cerebellum in the patient group, predicting a deficit of the fast learning system. This would explain why the cerebellar group was much slower to adapt and did not adapt to the extent of control participants, in line with previous work (Donchin et al., 2012). In contrast to control participants, error sensitivity of the slow system was not reduced in cerebellar participants after extended training, which made the slow state less resilient against washing out. Given the hypothesized association between the slow learning system and the DCN, reduced memory resilience could be the result of reduced DCN integrity. The cerebellar group may have been affected by reduced DCN integrity, since structure and function abnormalities of the DCN are common in patients with hereditary cerebellar ataxia (Stefanescu et al., 2015). Interestingly, lesions of the DCN have been linked to impaired long-term recovery and upper limb function after stroke and surgery (Konczak et al., 2005; Schoch et al., 2006), which we suggest could be due to reduced memory resilience. However, since the DCN were not imaged in this study, we cannot make conclusive statements about the relationship between memory resilience and DCN integrity.

4.3 What underlies increased retention rates?

While memory resilience was reduced in cerebellar participants, spontaneous recovery was still amplified after extended training. The modelling results suggest this was due to a shift towards more retention of the slow system (A_{Slow}) and not increased memory resilience. A similar shift towards higher retention rates of the slow system was also observed in control participants. Since this property of motor learning is still preserved in cerebellar participants, the mechanism underlying increased retention rates could be extra-cerebellar.

687 A possible candidate for such an extra-cerebellar mechanism is use-dependent plasticity.
688 When movements are repeatedly made towards the same area of the workspace, directional
689 movement biases are formed that shape consecutive movements (Diedrichsen et al., 2010).
690 Extended training towards the same target directions can therefore induce stronger movement
691 biases and result in additional spontaneous recovery. In our experiment, targets were spread
692 over a relatively limited area of the workspace (48°), so use-dependent movement biases were
693 likely to build (cf. experiment 4 McDougle et al., 2015). Thus, we suggest that elevated
694 spontaneous recovery after extended training in healthy participants is the result of two
695 separate effects: use-dependent learning, resulting in higher retention rates of the slow system,
696 and increased memory resilience, resulting in lower learning rates in the slow system. In
697 contrast, we suggest that the elevated spontaneous recovery in cerebellar patients reflects only
698 one of these effects: use-dependent learning, potentially an extra-cerebellar process.

699 *4.4 Could use-dependent plasticity be leveraged for cerebellar therapy?*

700 Prior work has found that intensive therapy programs are effective in reducing ataxia
701 symptoms in cerebellar participants (Ilg et al., 2009; Miyai et al., 2012). These therapy
702 programs were intensive, because patients were trained multiple times a week. Interestingly,
703 long-term gains of therapy were correlated with the training intensity after the intervention
704 period, as cerebellar patients that trained more at home retained a larger functional
705 improvement after 1-year follow-up (Ilg et al., 2010). In that sense, continued high intensity
706 therapy is a form of overlearning, since cerebellar patients continue training already learned
707 behavior. The gains after high intensity therapy could therefore be the result of use-dependent
708 learning as well. It should be noted however that the benefit of use-dependent learning during
709 therapy might be limited by disease progression (Donchin and Timmann, 2019). That is,
710 impaired learning from sensory-prediction errors due to cerebellar degeneration might also

disrupt other motor learning mechanisms when cerebellar disease is sufficiently far progressed.

Another possible application of our results is to see whether motor memory resilience can predict response to neurorehabilitation. Although evidence is still limited, there appears to be a link between motor learning deficits and the success of neurorehabilitation (Hatakenaka et al., 2012). Our modeling results suggest that healthy participants successfully reduce error sensitivity of the slow system while cerebellar patients do not. Thus, reduced memory resilience could be a sign of disease progression and patients with reduced memory resilience might benefit less from extended training than patients with relatively intact memory resilience. As such, motor memory resilience might help in identifying which cerebellar patients will respond best to intensive therapy.

4.5 Limitations

Several limitations have to be taken into account while interpreting the results of this study. Firstly, the two-state model with fixed learning and retention rates could not account for the full amount of early learning and the extent of spontaneous recovery. Only when two independent models were fit to the early and late phase of training did the model output accurately match behavior. Others have described rate changes of the two-state model, but mainly in the context of faster relearning (Coltman et al., 2019; Zarahn et al., 2008). Our results further indicate that model parameters likely vary between different phases of motor learning and fixed parameters cannot account for these variations.

Secondly, motor learning during reach adaptation experiments depends on multiple learning mechanisms (Haith and Krakauer, 2013), including learning from sensory prediction errors (Shadmehr et al., 2010), use-dependent learning (Diedrichsen et al., 2010), reinforcement learning (Galea et al., 2015) and strategic learning (Taylor et al., 2014). We only considered the effects of error-based learning and use-dependent learning on motor behaviors. While our

736 training paradigms were not developed to selectively engage reinforcement learning or
737 strategic learning, a differential effect of these learning mechanisms between paradigms
738 cannot be excluded. Furthermore, we only considered that error sensitivity of the slow state
739 changed due to reduced state estimation uncertainty, but it could be the result of other factors
740 as well. For instance, planning and execution noise correlate with learning rates (van der Vliet
741 et al., 2018), and the fast system might be temporally labile, while the slow system is
742 temporally stable (Sing et al., 2009).
743 Finally, though the modelling results of the gradual and long ITI paradigm are not discussed
744 in the present manuscript, the extended materials reveal that the learning and retention
745 parameters shift in these paradigms as well. However, since behaviorally the gradual and long
746 ITI paradigms are equivalent to the standard paradigm, it is difficult to infer the exact
747 implications of these parameter shifts in the current study.

748 *4.6 Conclusions*

749 The present study investigated the effect of slow learning paradigms on motor behavior. Of
750 the training paradigms tested, only overlearning elicited higher levels of spontaneous recovery
751 compared to standard learning. We suggest that enhanced motor retention was the result of
752 changes to memory resilience and use-dependent plasticity in control participants. Memory
753 resilience in cerebellar participants was diminished, which we suggest could be caused by
754 reduced DCN integrity. To our knowledge, this is the first time this deficit has been described
755 in cerebellar patients. We suggest that cerebellar patients might still benefit from extended
756 training through use-dependent learning.

5 References

Antonietti, A., Casellato, C., D'Angelo, E., and Pedrocchi, A. (2017). Model-Driven Analysis of Eyeblink Classical Conditioning Reveals the Underlying Structure of Cerebellar Plasticity and Neuronal Activity. IEEE Trans. Neural Netw. Learn. Syst. *28*, 2748–2762.

Casellato, C., Antonietti, A., Garrido, J.A., Ferrigno, G., D'Angelo, E., and Pedrocchi, A. (2015). Distributed cerebellar plasticity implements generalized multiple-scale memory components in real-robot sensorimotor tasks. Front. Comput. Neurosci. *9*.

Coltman, S.K., Cashaback, J.G.A., and Gribble, P.L. (2019). Both fast and slow learning processes contribute to savings following sensorimotor adaptation. J. Neurophysiol. *121*, 1575–1583.

Criscimagna-Hemminger, S.E., Bastian, A.J., and Shadmehr, R. (2010). Size of error affects cerebellar contributions to motor learning. J. Neurophysiol. *103*, 2275–2284.

Diedrichsen, J., and Zotow, E. (2015). Surface-Based Display of Volume-Averaged Cerebellar Imaging Data. PLOS ONE *10*, e0133402.

Diedrichsen, J., Balsters, J.H., Flavell, J., Cussans, E., and Ramnani, N. (2009). A probabilistic MR atlas of the human cerebellum. NeuroImage *46*, 39–46.

Diedrichsen, J., White, O., Newman, D., and Lally, N. (2010). Use-Dependent and Error-Based Learning of Motor Behaviors. J. Neurosci. *30*, 5159–5166.

Donchin, O., and Timmann, D. (2019). How to help cerebellar patients make the most of their remaining learning capacities. Brain *142*, 492–495.

Donchin, O., Rabe, K., Diedrichsen, J., Lally, N., Schoch, B., Gizewski, E.R., and Timmann, D. (2012). Cerebellar Regions Involved in Adaptation to Force Field and Visuomotor Perturbation. J. Neurophysiol. *107*, 134–147.

Fonteyn, E.M.R., Keus, S.H.J., Verstappen, C.C.P., Schöls, L., de Groot, I.J.M., and van de Warrenburg, B.P.C. (2014). The effectiveness of allied health care in patients with ataxia: a systematic review. J. Neurol. *261*, 251–258.

Galea, J.M., Mallia, E., Rothwell, J., and Diedrichsen, J. (2015). The dissociable effects of punishment and reward on motor learning. Nat Neurosci *18*, 597–602.

Gibo, T.L., Criscimagna-Hemminger, S.E., Okamura, A.M., and Bastian, A.J. (2013). Cerebellar motor learning: are environment dynamics more important than error size? J. Neurophysiol. *110*, 322–333.

Gomez, C.M., Thompson, R.M., Gammack, J.T., Perlman, S.L., Dobyns, W.B., Truwit, C.L., Zee, D.S., Clark, H.B., and Anderson, J.H. (1997). Spinocerebellar ataxia type 6: Gaze-evoked and vertical nystagmus, Purkinje cell degeneration, and variable age of onset. Ann. Neurol. *42*, 933–950.

Haith, A.M., and Krakauer, J.W. (2013). Model-Based and Model-Free Mechanisms of Human Motor Learning. In Progress in Motor Control, M.J. Richardson, M.A. Riley, and K. Shockley, eds. (New York, NY: Springer New York), pp. 1–21.

795 Hatakenaka, M., Miyai, I., Mihara, M., Yagura, H., and Hattori, N. (2012). Impaired Motor
796 Learning by a Pursuit Rotor Test Reduces Functional Outcomes During Rehabilitation of
797 Poststroke Ataxia. Neurorehabil. Neural Repair *26*, 293–300.

798 Herzfeld, D.J., Vaswani, P.A., Marko, M.K., and Shadmehr, R. (2014). A memory of errors in
799 sensorimotor learning. Science *345*, 1349–1353.

800 Hulst, T., van der Geest, J.N., Thürling, M., Goericke, S., Frens, M. a., Timmann, D., and
801 Donchin, O. (2015). Ageing shows a pattern of cerebellar degeneration analogous, but not
802 equal, to that in patients suffering from cerebellar degenerative disease. NeuroImage *116*,
803 196–206.

804 Ilg, W., Synofzik, M., Brötz, D., Burkard, S., Giese, M.A., and Schöls, L. (2009). Intensive
805 coordinative training improves motor performance in degenerative cerebellar disease.
806 Neurology *73*, 1823–1830.

807 Ilg, W., Brötz, D., Burkard, S., Giese, M.A., Schöls, L., and Synofzik, M. (2010). Long-term
808 effects of coordinative training in degenerative cerebellar disease. Mov. Disord. *25*, 2239–
809 2246.

810 Ilg, W., Bastian, A.J., Boesch, S., Burciu, R.G., Celnik, P., Claa??en, J., Feil, K., Kalla, R.,
811 Miyai, I., Nachbauer, W., et al. (2014). Consensus paper: Management of degenerative
812 cerebellar disorders. Cerebellum *13*, 248–268.

813 Jayadev, S., and Bird, T.D. (2013). Hereditary ataxias: Overview. Genet. Med. *15*, 673–683.

814 Joiner, W.M., and Smith, M.A. (2008). Long-Term Retention Explained by a Model of Short-
815 Term Learning in the Adaptive Control of Reaching. J. Neurophysiol. *100*, 2948–2955.

816 Kim, S., Oh, Y., and Schweighofer, N. (2015). Between-Trial Forgetting Due to Interference
817 and Time in Motor Adaptation. PLOS ONE *10*, e0142963.

818 Konczak, J., Schoch, B., Dimitrova, A., Gizewski, E., and Timmann, D. (2005). Functional
819 recovery of children and adolescents after cerebellar tumour resection. Brain *128*, 1428–1441.

820 Kording, K.P., Tenenbaum, J.B., and Shadmehr, R. (2007). The dynamics of memory as a
821 consequence of optimal adaptation to a changing body. Nat. Neurosci. *10*, 779–786.

822 Kruschke, J. (2010). Doing Bayesian Data Analysis.

823 Mariotti, C., Fancellu, R., and Donato, S. (2005). An overview of the patient with ataxia. J.
824 Neurol. *252*, 511–518.

825 Marko, M.K., Haith, A.M., Harran, M.D., and Shadmehr, R. (2012). Sensitivity to prediction
826 error in reach adaptation. J. Neurophysiol. *108*, 1752–1763.

827 Maschke, M., Gomez, C.M., Ebner, T.J., and Konczak, J. (2004). Hereditary cerebellar ataxia
828 progressively impairs force adaptation during goal-directed arm movements. J. Neurophysiol.
829 *91*, 230–238.

830 Matilla-Dueñas, A., Ashizawa, T., Brice, A., Magri, S., McFarland, K.N., Pandolfo, M., Pulst,
831 S.M., Riess, O., Rubinsztein, D.C., Schmidt, J., et al. (2014). Consensus Paper: Pathological

832 Mechanisms Underlying Neurodegeneration in Spinocerebellar Ataxias. The Cerebellum *13*,
833 269–302.

834 McDougle, S.D., Bond, K.M., and Taylor, J. a. (2015). Explicit and Implicit Processes
835 Constitute the Fast and Slow Processes of Sensorimotor Learning. J. Neurosci. *35*, 9568–
836 9579.

837 Medina, J.F., Garcia, K.S., and Mauk, M.D. (2001). A Mechanism for Savings in the
838 Cerebellum. J. Neurosci. *21*, 4081–4089.

839 Miyai, I., Ito, M., Hattori, N., Mihara, M., Hatakenaka, M., Yagura, H., Sobue, G., and
840 Nishizawa, M. (2012). Cerebellar ataxia rehabilitation trial in degenerative cerebellar
841 diseases. Neurorehabil. Neural Repair *26*, 515–522.

842 Oldfield, R.C. (1971). The assessment and analysis of handedness: the Edinburgh inventory.
843 Neuropsychologia *9*, 97–113.

844 Plummer, M. (2003). JAGS: A program for analysis of Bayesian graphical models using
845 Gibbs sampling. Proc. 3rd Int. Workshop Distrib. Stat. Comput. DSC 2003 20–22.

846 Rabe, K., Livne, O., Gizewski, E.R., Aurich, V., Beck, a, Timmann, D., and Donchin, O.
847 (2009). Adaptation to visuomotor rotation and force field perturbation is correlated to
848 different brain areas in patients with cerebellar degeneration. J. Neurophysiol. *101*, 1961–
849 1971.

850 Schlerf, J.E., Xu, J., Klemfuss, N.M., Griffiths, T.L., and Ivry, R.B. (2013). Individuals with
851 cerebellar degeneration show similar adaptation deficits with large and small visuomotor
852 errors. J. Neurophysiol. *109*, 1164–1173.

853 Schmahmann, J.D., and Sherman, J.C. (1998). The cerebellar cognitive affective syndrome.
854 Brain *121*, 561–579.

855 Schmitz-Hübsch, T., Du Montcel, S.T., Baliko, L., Berciano, J., Boesch, S., Depondt, C.,
856 Giunti, P., Globas, C., Infante, J., Kang, J.S., et al. (2006). Scale for the assessment and rating
857 of ataxia. Neurology *66*, 1717–1720.

858 Schoch, B., Dimitrova, A., Gizewski, E.R., and Timmann, D. (2006). Functional localization
859 in the human cerebellum based on voxelwise statistical analysis: A study of 90 patients.
860 NeuroImage *30*, 36–51.

861 Scoles, D.R., Meera, P., Schneider, M.D., Paul, S., Dansithong, W., Figueroa, K.P., Hung, G.,
862 Rigo, F., Bennett, C.F., Otis, T.S., et al. (2017). Antisense oligonucleotide therapy for
863 spinocerebellar ataxia type 2. Nature *544*, 362–366.

864 Shadmehr, R., Smith, M. a, and Krakauer, J.W. (2010). Error correction, sensory prediction,
865 and adaptation in motor control. Annu. Rev. Neurosci. *33*, 89–108.

866 Sing, G., Najafi, B., Adewuyi, A., and Smith, M. (2009). A mechanism for the spacing effect:
867 Competitive inhibition between adaptive processes explains the increase in motor skill
868 retention associated with prolonged inter-trial spacing. Adv. Comput. Mot. Control Chic. IL.

869 Smith, M.A., Ghazizadeh, A., and Shadmehr, R. (2006). Interacting Adaptive Processes with
870 Different Timescales Underlie Short-Term Motor Learning. PLoS Biol *4*, e179.

871 Stefanescu, M.R., Dohnalek, M., Maderwald, S., Thürling, M., Minnerop, M., Beck, A.,
872 Schlamann, M., Diedrichsen, J., Ladd, M.E., and Timmann, D. (2015). Structural and
873 functional MRI abnormalities of cerebellar cortex and nuclei in SCA3, SCA6 and Friedreich's
874 ataxia. Brain *138*, 1182–1197.

875 Taig, E., Küper, M., Theysohn, N., Timmann, D., and Donchin, O. (2012). Deficient use of
876 visual information in estimating hand position in cerebellar patients. J. Neurosci. Off. J. Soc.
877 Neurosci. *32*, 16274–16284.

878 Taylor, J.A., Klemfuss, N.M., and Ivry, R.B. (2010). An Explicit Strategy Prevails When the
879 Cerebellum Fails to Compute Movement Errors. The Cerebellum *9*, 580–586.

880 Taylor, J.A., Krakauer, J.W., and Ivry, R.B. (2014). Explicit and Implicit Contributions to
881 Learning in a Sensorimotor Adaptation Task. J. Neurosci. *34*, 3023–3032.

882 Therrien, A.S., Wolpert, D.M., and Bastian, A.J. (2016). Effective reinforcement learning
883 following cerebellar damage requires a balance between exploration and motor noise. Brain
884 *139*, 101–114.

885 Timmann, D., Konczak, J., Ilg, W., Donchin, O., Hermsdörfer, J., Gizewski, E.R., and
886 Schoch, B. (2009). Current advances in lesion-symptom mapping of the human cerebellum.
887 Neuroscience *162*, 836–851.

888 Trouillas, P., Takayanagi, T., Hallett, M., Currier, R.D., Subramony, S.H., Wessel, K., Bryer,
889 A., Diener, H.C., Massaquoi, S., Gomez, C.M., et al. (1997). International Cooperative Ataxia
890 Rating Scale for pharmacological assessment of the cerebellar syndrome. J. Neurol. Sci. *145*,
891 205–211.

892 Tseng, Y.-W., Diedrichsen, J., Krakauer, J.W., Shadmehr, R., and Bastian, A.J. (2007).
893 Sensory Prediction Errors Drive Cerebellum-Dependent Adaptation of Reaching. J.
894 Neurophysiol. *98*, 54–62.

895 van der Vliet, R., Frens, M.A., de Vreede, L., Jonker, Z.D., Ribbers, G.M., Selles, R.W., van
896 der Geest, J.N., and Donchin, O. (2018). Individual Differences in Motor Noise and
897 Adaptation Rate Are Optimally Related. Eneuro *5*, ENEURO.0170-18.2018.

898 Wei, K. (2010). Uncertainty of feedback and state estimation determines the speed of motor
899 adaptation. Front. Comput. Neurosci.

900 Williams, E. (1949). Experimental designs balanced for the estimation of residual effects of
901 treatments. Aust. J. Chem. *2*, 149–168.

902 Zarahn, E., Weston, G.D., Liang, J., Mazzoni, P., and Krakauer, J.W. (2008). Explaining
903 savings for visuomotor adaptation: linear time-invariant state-space models are not sufficient.
904 J. Neurophysiol. *100*, 2537–2548.

905